Russian Chemical Reviews **70** (9) 777 – 790 (2001) © 2001 Russian Academy of Sciences and Turpion Ltd

DOI 10.1070/RC2001v070n09ABEH000670

Magnetic properties of complex oxides $LiMO_2$ (M = Sc – Ni) with different types of cationic ordering

D G Kellerman

Contents

I.	Introduction	777
II.	Structures of $LiMO_2$ oxides	777
III.	Magnetic properties of $LiMO_2$ oxides	781
IV.	Structure and magnetic properties of $LiM_{1-x}M'_xO_2$ solid solutions	785
V.	Conclusion	788

Abstract. The crystal structures and magnetic properties of complex oxides of the $LiMO_2$ series (M = Sc – Ni) and of solid solutions they form are described. Although the structures of the oxides are all derived from the NaCl structure, their magnetic properties are fairly diverse and depend on the type of cationic ordering. Primary attention is given to the oxides with layered structures in which the degree of ordering is a variable. The bibliography includes 225 references.

I. Introduction

During the past 15 years, compounds with the general formula of $LiMO_2$, where M is a transition 3*d* metal, have actively been explored, and the interest in them is not lost up to date. First of all, this is related to the prospects of considering many $LiMO_2$ complex oxides as promising cathodic materials for chemical power sources.[1–3] These prospects are usually determined by such properties as a high positive potential, small molecular mass and structural stability during electrochemical intercalation and deintercalation

$$LiMO_2 \rightleftharpoons Li_{1-x}MO_2 + x\,Li^+ + x\,e^-.$$

Besides this applied aspect, interesting magnetic properties of $LiMO_2$ complex oxides draw the attention of many theoreticians and researchers.[4] These oxides include antiferromagnetic, ferromagnetic, paramagnetic, diamagnetic, weak ferromagnetic materials, *etc*. The magnetic properties of $LiMO_2$ oxides are largely determined by the type of superstructures they form. The whole spectrum of structures found in $LiMO_2$ is based on the rock-salt structure, the deviations being determined by the way the cations are distributed over the positions of this basal structure. This distribution can either be random or ordered, the latter giving rise to the formation of a superstructure. In solid solutions of complex oxides, the type and the degree of ordering can change depending on the component concentrations. This is why compounds for which the degree of structural ordering (η) varies as a function of synthetic conditions, which entails profound changes in magnetic structures, are of particular interest. In this review, the studies in which the magnetic properties of $LiMO_2$ compounds and solid solutions based on them are correlated with the peculiarities of their crystal structures are analysed. Most of numerous electrochemical studies are beyond the scope of this review, these being surveyed elsewhere.[3–5]

D G Kellerman Institute of Solid State Chemistry, Urals Branch of the Russian Academy of Sciences, ul. Pervomaiskaya 91, 620219 Ekaterinburg, Russian Federation. Fax (7-343) 274 44 95. Tel. (7-343) 249 34 42. E-mail: kellerman@ihim.uran.ru

Received 26 March 2001
Uspekhi Khimii **70** (9) 874 – 889 (2001); translated by T Ya Safonova

II. Structures of $LiMO_2$ oxides

The crystal structures of $LiMO_2$ complex oxides derive from the NaCl structure and differ from one another only in the way the cations of alkali and transition metals are distributed over the planes of the basal cubic lattice. When lithium and transition-metal ions occupy severally the alternating (111) planes of the sodium chloride cubic lattice, layered structures characterised by a high diffusion mobility of alkali-metal atoms are formed. Hence, in such compounds as, *e.g.*, $LiCoO_2$ and $LiNiO_2$, deep and reversible electrochemical intercalation of lithium can occur which attracts the attention of scientists. The quest for a wide array of new compounds with the layered structures favourable for electrochemical processes stimulates the development of the methods for the preparation of metastable $LiMO_2$ modifications. For this purpose, low-temperature methods which involve precursor synthesis and ion-exchange processes, chemical and electrochemical intercalation, etc. are used. Usually, these phases lose their stabilities with an increase in temperature and transform into stable modifications.

The $LiMO_2$ compounds preferentially form three structural types. The first structure represents a disordered cubic lattice of α-$LiFeO_2$ (NaCl), the second structure of the α-$NaFeO_2$ type represents a trigonal superlattice on the basis of the NaCl structure and the third compound represents a spinel in which transition-metal and lithium atoms occupy, correspondingly, the 16*a* and 16*b* positions. The effects of the size and the charge of a transition-metal ion on the formation of a particular lattice type have been discussed.[6] As was shown by calculation, if the ionic radii of alkali and transition metals are close, the random distribution of ions over the positions corresponds to the state with the minimum energy, *viz*., the cubic lattice of α-$LiFeO_2$. With an increase in the differences in the ionic sizes, the probability of formation of the α-$NaFeO_2$-type layered structure also increases, which is favoured by lower charges of transition-metal ions. The low stability of spinel phases (*e.g.*, the low-temperature $LiCoO_2$ phase), which exist only in very narrow temperature and pressure intervals is explained by the fact that their origination is governed by kinetic factors rather than by thermodynamic ones.

$LiScO_2$ represents a nonconducting white powder under ordinary conditions. A review of the structural data one can see in Ref. 4. $LiScO_2$ was first described in 1959 (Ref. 7). X-Ray diffraction studies carried out for both single crystals[8] and powders[9] and Mössbauer studies of Fe^{3+} impurity centres in $LiScO_2$ (see Refs 10, 11) have shown that the perfect ordering of Sc^{3+} and Li^+ cations in the basal NaCl structure produces a superlattice with $I4_1/amd$ symmetry ($a = 4.18$, $c = 9.30$ Å), which is similar to the superlattice of totally ordered γ-$LiFeO_2$ phase. This structure is characterised by the atoms of transition and alkali metals regularly occupying the alternate positions along the tetragonal c axis.

Yet another approach to the description of the $LiScO_2$ structure is known.[12] According to experimental results,[12] the oxygen octahedra which enclose lithium ions are shown to be distorted in a such way as if lithium represented a Jahn–Teller ion (four short and two long Li–O distances). The concept of distorted anatase seems to describe the $LiScO_2$ structure more precisely than the model of a tetragonally ordered NaCl modification.

$LiTiO_2$ has a completely disordered cubic structure of the NaCl type ($a = 4.140$ Å).[13, 14] Extensive information on $LiTiO_2$ is cited in Ref. 4. Low-temperature chemical lithiation of $LiTi_2O_4$ spinel gave rise to a modification of $LiTiO_2$.[15] X-Ray diffraction patterns of this phase virtually did not differ from those of the parent spinel. Using the neutron diffraction technique, it was shown[16] that the formation of $LiTiO_2$ ($Li_2Ti_2O_4$) ($a = 8.3756$ Å) is accompanied by transposition of lithium from tetrahedral sites to octahedral ones unoccupied in the parent spinel. Thus, the titanium and lithium ions in the metastable phase are distributed over the positions 16c and 16d, respectively, of the $Fd3m$ space group, and a superstructure of the atacamite type is formed.[17] Heating above 920 K results in irreversible transition of the $Li_2Ti_2O_4$ spinel into a stable disordered cubic phase of $LiTiO_2$.[15] This transition appears to occur in several steps, because DSC (differential scanning calorimetry) revealed three endothermic effects (in total, 950 cal mol^{-1} were liberated).[18]

$LiVO_2$ represents a black powder. It was described for the first time in 1954 (Ref. 19). This compound is isostructural to the hexagonal α-$NaFeO_2$. Generally, such a structure is typical of this class of compounds (Fig. 1). It is formed by the ions of alkali and transition metals ordered in parallel (111) planes of the NaCl cubic lattice. In the ordered structure, all vanadium ions have six-fold oxygen coordination, the V–O distances are equal to 1.987 Å. At 450 K, a phase transition occurs in $LiVO_2$,[13, 20–22] which is accompanied by pronounced changes in the unit cell volume and interatomic distances [$a = 2.837$, $c = 14.775$, V–O = 1.98, V–V = 2.84 Å at 300 K; $a = 2.913$, $c = 14.640$, V–O = 2.02, V–V = 2.91 Å at 550 K for $Li_{0.7}VO_2$ (see Ref. 23)], although the main structural motif remains unchanged. A substantial temperature hysteresis was observed. During the transition, the enthalpy changed by 50–1000 cal mol^{-1} (see Ref. 22). It was assumed[24] that at room temperature vanadium ions are combined in V_3 trimers which disintegrate during the phase transition. The formation of trimers was confirmed experimentally. Thus, the structure of $Li_{0.8}VO_2$ single crystals prepared by the flux method (see Ref. 26) was analysed in detail using X-ray diffraction and EXAFS techniques.[25] It was shown that vanadium ions are shifted by 0.160 Å from the positions they should occupy in the perfect hexagonal structure. Probably, the symmetry of the low-temperature phase differs from the $R\bar{3}m$ symmetry as followed from the presence of very weak additional reflexes in the X-ray patterns of this phase ($a' = a\sqrt{3}$, $c' = c$).[23]

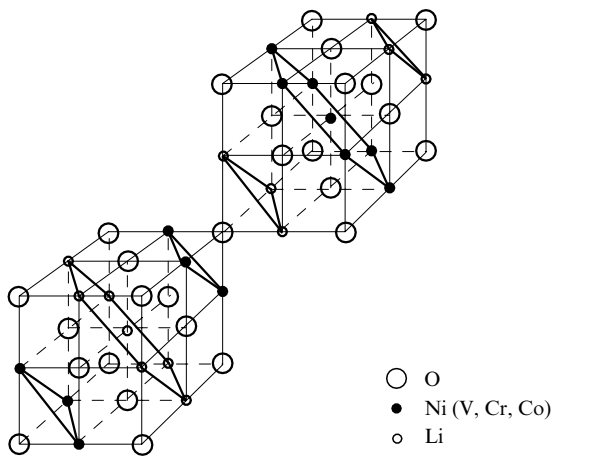


Figure 1. Schematic representation of the formation of layered structures for $LiVO_2$, $LiCrO_2$, $LiCoO_2$ and $LiNiO_2$ as a result of cationic ordering in the NaCl-type cubic lattice.

It was shown that stoichiometric $LiVO_2$ can be transformed into $Li_{1-x}VO_2$ phases by both chemical and electrochemical deintercalation.[27, 28] Studies on the structure of deintercalated vanadates showed that the removal of lithium from the layered structure for $x \geqslant 0.3$ results in redistribution of vanadium ions. For example, in $Li_{0.22}VO_2$, approximately one third of vanadium ions occupy the octahedral positions in Li layers, which favours stabilisation of the cubic structure. With increasing temperature, the $Li_{1-x}VO_2$ phase becomes unstable, and its disproportionation can proceed by two routes[29]

$$Li_{1-x}VO_2 \longrightarrow (1-2x)\,LiVO_2 + x\,LiV_2O_4,$$

$$Li_{1-x}VO_2 \longrightarrow (1-8x)\,LiVO_2 + 8x\,Li_{0.875}VO_2.$$

The coexistence of hexagonal and cubic phases was established.[30]

At high pressures, another polymorphous modification of $LiVO_2$ with a superlattice of the atacamite type was obtained.[31] Heating above 700 K resulted in irreversible transition of this phase into a stable hexagonal form.

$LiCrO_2$ prepared by ceramic technology represents a green powder with a layered trigonal structure of α-$NaFeO_2$ ($a = 2.88$, $c = 14.6$ Å). Like $LiVO_2$, the $LiCrO_2$ oxide was first prepared and described in 1954 (Ref. 19). Single crystals of $LiCrO_2$ were grown by the flux method.[32] In contrast to most $LiMO_2$ compounds, deintercalation of lithium from $LiCrO_2$ is hindered; however, under hydrothermal conditions, the ion-exchange reaction is possible, which results in the formation of an isostructural phase of $HCrO_2$.[33]

$LiMnO_2$ in the form of a brown powder (orthorhombic unit cell) was first synthesised with the aim of studying the $Li_xMn_{1-x}O$ system.[34] The crystal structure of $LiMnO_2$ was studied in more detail for polycrystalline material[35] and single crystals[36], the latter being obtained by the hydrothermal method.[37] A number of structural peculiarities of orthorhombic $LiMnO_2$ compared with other $LiMO_2$ complex oxides[38] are apparently caused by the Jahn–Teller effect.

The orthorhombic lattice of $LiMnO_2$ ($a = 2.805$, $b = 5.757$, $c = 4.527$ Å), $Pmmn$ (see Ref. 36) also represents one of the versions of the NaCl basal structure ordering (Fig. 2). The MnO_6 octahedra are substantially distorted due to the Jahn–Teller effect. Two long distances along the b axis (2.291 Å) and two pairs of almost identical equatorial distances, *viz.*, 1.920 and 1.937 Å, were observed. In each (001) plane, cations of one type are arranged in chains along either ⟨100⟩ (orthorhombic) or ⟨110⟩ (cubic) directions. In alternate (001) planes, the chains retain their orientation with respect to the upper and lower planes, but are shifted forming the ABA packing along the c axis. Compared to the hypothetical cubic lattice with a parameter a', the parameters of the real lattice are as follows: $a = (1/2)\sqrt{2}a'$, $b = \sqrt{2}a'$ and $c = a'$.

Considerable anisotropy of the thermal expansion coefficient was observed[39] at temperatures < 300 K. The thermal expansion coefficient did not exceed 10^{-7} K^{-1} in the directions a and b and was 3.7×10^{-6} K^{-1} in the direction c.

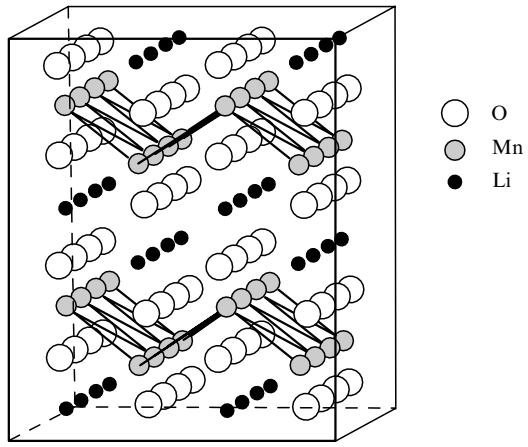


Figure 2. Crystal structure of $LiMnO_2$.

Studies on the morphological peculiarities of orthorhombic $LiMnO_2$ synthesised by a conventional ceramic procedure (sintering of an Mn_2O_3 + LiOH mixture at 1073 K in an inert atmosphere) revealed the presence of certain cationic disordering, namely, the existence of defects of the Li_{Mn} and Mn_{Li} types.[40] The degree of disordering (3% – 12%) was attributed to the preset excess or deficiency of LiOH. Scanning electron microscopy showed that the sizes and shapes of grains also depended on the LiOH content in the reaction mixture. The deficiency of lithium favoured the formation of fine and size-uniform grains, whereas excess of lithium resulted in a wide scatter of the grains both in sizes and shapes. It was the former modification that demonstrated good characteristics in the electrochemical process.[41] The stacking faults in orthorhombic $LiMnO_2$ with a small ($d \approx 0.3$ μm) grain size were studied in detail.[42] It was concluded that these represent monoclinic interstitial layers between the orthorhombic blocks. The portion of such defects was 1% – 6%, which correlated well with the degree of cationic disordering.

The existence of a low-temperature modification of $LiMnO_2$ with a tetragonal structure, which was obtained by chemical lithiation of $LiMn_2O_4$ spinel: $a = 5.662$, $c = 9.274$ Å, $I4_1/amd$, $Z = 8$, was reported.[43,44] Above 500 °C, the tetragonal phase transformed into the stable orthorhombic phase.

Recently, yet another metastable low-temperature modification of $LiMnO_2$ has attracted great interest. This phase was first synthesised in 1996 (Ref. 45). The phase has a monoclinic lattice ($C2/m$, $a = 5.4387$, $b = 2.8086$, $c = 5.3878$ Å, β = 116 °). For its synthesis, the ion-exchange method was applied in which layered α-$NaMnO_2$ was used as the precursor. The product also exhibited a layered structure. In addition, it was noted[46,47] that the ion-exchange reaction can also proceed in a mixture of γ-MnOOH and $LiOH \cdot H_2O$. The lower symmetry of the layered $LiMnO_2$ modification compared, for instance, with layered $LiCoO_2$ was associated with the strong Jahn–Teller effect for Mn^{3+} ions (see Ref. 45). As was shown by the results of X-ray diffraction analysis and neutron diffraction,[45,48,49] the Li-layers of the layered $LiMnO_2$ modification contain 3% – 9% of manganese ions. An electron-diffraction study in a convergent beam[50] have shown that a typical specimen synthesised by the ion-exchange method contains, in addition to layered $LiMnO_2$, an admixture of a tetragonal spinel phase of $Li_2[Mn_2]O_4$ and traces of orthorhombic $LiMnO_2$. The following atomic planes and directions were also shown[50] to be equivalent for the spinel and layered phases:

$$(200)_{lay} \equiv (222)_{sp}$$

$$(020)_{lay} \equiv (4\text{-}40)_{sp}$$

$$[001]_{lay} \equiv [11\text{-}2]_{sp}$$

A comparative analysis of the stability of orthorhombic and monoclinic layered structures of $LiMnO_2$ was carried out.[51] The calculations have shown that the antiferromagnetic exchange coupling of Mn^{3+} ions plays a substantial role in stabilisation of the orthorhombic structure; and, therefore, stabilisation of the layered structure requires that manganese was partly replaced by elements that weaken this interaction. The elements Al, Co, Cr, V, Ti, Mo, Mg, Nb, Zn and Pd can serve as the dopants.

In the Li–Mn–O system, yet another monoclinic phase designated as m-Li_xMnO_2 ($x = 0.2 – 0.3$) was detected and identified.[52] It can be obtained by durable sintering of intimately mixed β-MnO_2 and LiOH at 420 K. According to the results of X-ray diffraction analysis, the new phase has a primitive monoclinic unit cell ($a = 9.38$, $b = 5.65$, $c = 4.906$ Å, β = 102.2 °) and is stable up to 820 K.

In a thermobaric treatment ($P = 6.5$ GPa, $T = 100$ K) of orthorhombic $LiMnO_2$, a totally disordered phase with the rock-salt structure ($a = 4.1658$ Å) was obtained. According to crystallographic data, no structural distortions caused by the Jahn–Teller effect were observed.[4]

$LiFeO_2$ exists in several polymorphous modifications (Fig. 3). A disordered structure of cubic α-$LiFeO_2$ is identical to that of NaCl ($a = 4.158$ Å).[53] The structure of $LiFeO_2$ represents a rare example of structures in which two different cations occupy the same positions.[54,55] The results of electron-microscopic studies have shown[56,57] that the α-$LiFeO_2$ cubic structure involves the elements of the short-range order. For γ-$LiFeO_2$, an ordered tetragonal structure similar to that of $LiScO_2$ is typical ($a = 4.057$, $c = 8.759$ Å).[58] Apparently, the metastable β-$LiFeO_2$ modification is intermediate between α- and γ-phases. Discrepant opinions were advanced on the β-$LiFeO_2$ structure: some authors (see, *e.g.*, Ref. 53) claim the existence of a body-centred tetragonal unit cell, while others believe it to be monoclinic.[59,60] The monoclinic structure of the β-phase was confirmed by electron microscopy[56] ($C2/c$, $a = 8.571$, $b = 11.59$, $c = 5.147$ Å, β = 145.70 °, $Z = 8$). The tetragonal structure exhibits no ordering in the distribution of cations over the positions. In contrast, the monoclinic phase is ordered.

Detailed studies[53,61] have detected the transition of α-$LiFeO_2$ first to β-$LiFeO_2$ at $T > 570$ K and further to the ordered γ-$LiFeO_2$ phase at $T > 870$ K. The latter phase transforms back into the disordered α-modification with further increase in temperature (> 920 K). The transitions proceeded slowly and depended on the sample's prehistory.

Currently, many efforts are concentrated on the synthesis of metastable modifications of $LiFeO_2$ with layered structures. For

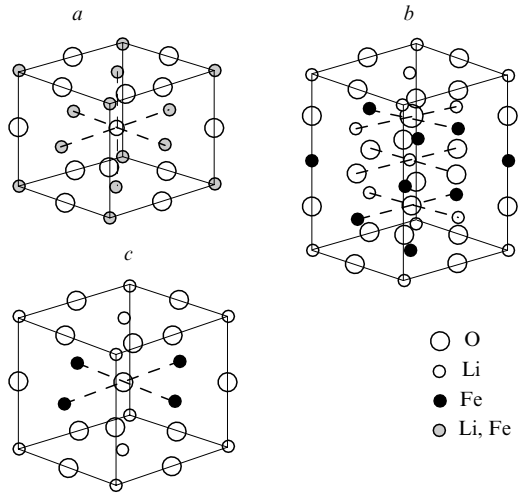


Figure 3. Structural modifications of $LiFeO_2$; (*a*) is the cubic α-phase, (*b*) is the tetragonal β-phase and (*c*) is the tetragonal γ-phase (1/2 of the unit cell is shown).

example, the preparation of $LiFeO_2$, the corrugated layered structure of which is similar to that of a stable orthorhombic modification of $LiMnO_2$, was described.[62] The synthesis involved the ion exchange reaction between γ-FeOOH and $LiOH \cdot H_2O$. The reaction was carried out under hydrothermal conditions at 370 – 520 K. The structure of the phase obtained was noted to resemble very closely that of the original γ-FeOOH. The transition from γ-FeOOH to $LiFeO_2$ presumes a shift of corrugated layers by 1/2 along the *b* direction. According to the X-ray diffraction studies, the lattice parameters of $LiFeO_2$ are $a = 4.0610(5)$, $b = 2.9621(5)$ and $c = 6.0319(11)$ Å. Yet another orthorhombic structure of the goethite type with the parameters $a = 9.677(5)$, $b = 2.934$ and $c = 5.005$ Å, *Pmna* was also synthesised by using an ion-exchange reaction (carried out in an ethanolic solution, in contrast to the previous reaction).[63] It is interesting that at certain Li to Fe ratios, a totally disordered cubic modification of α-$LiFeO_2$ ($a = 4.161$ Å, *Fm3m*) can be obtained by this method,[64] its conventional synthesis requires high temperatures.

The ion-exchange reaction of $NaFeO_2$ in a lithium chloride melt resulted in $LiFeO_2$ with a layered trigonal structure of α-$NaFeO_2$, which is typical of this class of compounds.[65] The degree of cationic ordering was found to depend on the ordering of the precursor phase.

In addition to metastable forms of $LiFeO_2$ discussed above, yet another low-temperature modification, *viz*., a phase with a tunnel structure was documented.[66] However, this has not been described in detail in further publications.

$LiCoO_2$ is usually obtained at 1200 – 1300 K as a black powder from cobalt oxide and lithium carbonate. This phase is referred to as a high-temperature (HT) one. It is thermally stable up to 1120 K.[67] According to results of neutron diffraction studies,[68] HT-$LiCoO_2$ has a perfectly ordered structure of the α-$NaFeO_2$ type ($R\bar{3}m$) with the cell parameters $a = 2.8166$ and $c = 14.052$ Å.[69] The $LiCoO_2$ structure was studied for single crystals obtained by the flux method.[70] The layered structure of HT-$LiCoO_2$ is very stable and, as was shown by calculations,[71] the order – disorder transition can occur only at ~5100 K. This is substantially higher than the melting point, which makes such a transition practically unfeasible. On the other hand, according to calculations,[72] the use of high pressures can stimulate the transition with the formation of a cubic phase.

Synthesis at temperatures below 700 K produces a low-temperature (LT) phase with a structure somewhat different from that of HT-$LiCoO_2$.[73 – 81] According to the results of neutron diffraction analysis,[75] nearly 6% of lithium sites in LT-$LiCoO_2$ are occupied by cobalt. The phase formed upon deintercalation of lithium from LT-$LiCoO_2$ (Li_xCoO_2; $1 \geqslant x \geqslant 0.5$) can be described[77] either as a spinel modification ($Fd\bar{3}m$) in which up to 80% of lithium atoms occupy tetrahedral positions[74] or a phase with the trigonal layered structure ($R\bar{3}m$). NMR studies[82] are in favour of the second version, because the substantial structural disordering observed by this method corresponds to the second co-ordination sphere of lithium. Hence, the nearest neighbouring of lithium remains octahedral so that LT-$LiCoO_2$ may be considered as a partly disordered trigonal structure based on NaCl. A different opinion on this problem has been advanced.[83] Based on the combined use of transmission electron microscopy and X-ray diffraction analysis, it was concluded that the structure of LT-$LiCoO_2$ may be considered as an intermediate between the structures of perfect spinel and the layered modification.

A number of studies dealt with the phase transitions that occur both in HT-[84 – 86] and LT-$LiCoO_2$[75 – 77] during electrochemical deintercalation of these compounds. The stabilities of the phases obtained were calculated,[87, 88] and the phase diagram of Li_xCoO_2 was constructed.

The completely deintercalated layered phase of CoO_2 ($a = 2.822$, $c = 14.29$ Å) was first isolated and described in 1997 (Ref. 89). Unexpectedly, it was found that despite the structural disordering processes that occur during electrochemical deintercalation the product exhibited a very high degree of structural ordering. Several metastable polymorphous modifications were formed upon electrochemical deintercalation of Li_xCoO_2[90] synthesised from $Na_{0.7}CoO_2$ by ion-exchange.[91] Depending on the depth of the deintercalation process, the mode of CoO_6 octahedra packing changed.

In studies of phase transitions that occur during the chemical extraction of lithium from $LiCoO_2$ with the formation of $Li_{0.5}CoO_2$ it was found[92] that a common hexagonal structure is retained only up to the $Li_{0.92}CoO_2$ composition. For deeper extraction of lithium, a second, also hexagonal phase appears, which becomes the only phase present starting from the $Li_{0.79}CoO_2$ composition. The hexagonal structures differ in the *c*/*a* ratio, which is substantially higher for the second phase.

$LiNiO_2$ with a structure similar to that of α-$NaFeO_2$ ($a = 2.878$, $c = 14.19$ Å) was described for the first time in 1953 (Ref. 93). This oxide is isostructural to $LiCoO_2$ and $LiVO_2$. The distribution of atoms over the positions is as follows: Ni(3*a*) (0, 0, 0); Li(3*b*) (0, 0, 1/2); O(6*c*) (0, 0, 1/4) (0, 0, −1/4). The ratio $c/a = 4.93$ indicates the presence of an almost perfect face-centred cubic sublattice of oxygen, for which $c/a = 2\sqrt{6} = 4.90$. An EXAFS study of the Jahn – Teller co-operative effect has shown that two long (2.09 Å) and four short (1.91 Å N – O distances are present as a result of local distortion in NiO_6 octahedra.[94 – 95]

The layered $LiNiO_2$ oxide is traditionally considered as an end member of the series of $Li_xNi_{1-x}O$ solid solutions. The cationic ordering that takes place with increasing concentration of lithium in Li_xNiO_2 is well known and was discussed in a number of publications.[96] The disordered phase ($x < 0.56$) is isostructural to NiO (NaCl type), and the formation of a layered structure involves the ordering of ions of transition and alkali metals in alternate (111) planes of the NaCl-type cubic lattice, which is accompanied by lowering of the symmetry to trigonal. Due to the close radii of Ni^{3+} and Li^+ ions, the degree of ordering of cations over the positions in the alternate planes (η) can vary widely even for an invariant transition-to-alkali metal ratio. For example, the synthesis and properties of virtually stoichiometric $LiNiO_2$ with $0 \leqslant \eta \leqslant 1$ were described.[97, 98] The structural order $\eta = 0$ corresponds to cubic $LiNiO_2$ prepared by quenching of $LiNiO_2$ with $\eta = 1$ from a temperature of 1200 K.[97] The quenched phase is metastable; hence, the ordering process can occur at temperatures above 600 K.

The temperature of the order → disorder transition (layered → cubic structure) is 1020 K.[99] The transition proceeds slowly and is not completely reversible.

The difficulties of synthesising the stoichiometric $LiNiO_2$ were associated with the loss of lithium during sintering.[100 – 102] In this case, the parameter of cubic or trigonal cell depended linearly on the value of *x* in $Li_xNi_{1-x}O$.[96] Different versions of the synthesis, which allow one to minimise lithium losses, were described.[103]

It is of note that even upon annealing for a long time at sufficiently high temperatures (1100 K) $Li_xNi_{1-x}O$ is characterised by a heterogeneous bulk composition.[104] The procedure of refining of structural data turned out to be more efficient being carried out within the framework of a multiphase system rather than a 'single-phase' one.

The cationic distribution in nonstoichiometric $Li_{1-x}Ni_{1+x}O_2$ solutions was studied by X-ray diffraction analysis.[105] It was confirmed that, with an increase in *x*, the degrees of occupation of 3*a* and 3*b* positions by lithium (nickel) ions approach one another, which results in their random distribution for $x \geqslant 0.4$.

Two models of cationic distribution in $Li_{1-x}Ni_{1+x}O_2$ exist. According to the first model, superstoichiometric nickel occupies free sites in lithium layers, and the oxide can be described by the formula $[Li_{1-x}Ni_x][Ni]O_2$.[106] The second model assumes partial mixing of cations in both sites; in this case, the oxide has the following formula: $[Li_{1-x-\delta}Ni_{x+\delta}][Ni_{1-\delta}Li_\delta]O_2$.[105, 106] If the oxide composition approaches stoichiometric, then the first model is assumed[107] to be more probable.

It should be noted that the nickel that occupies 3*a* positions in the nickel sublattice of $Li_{1-x}Ni_{1+x}O_2$ corresponds predominantly to the Ni^{3+} state, whereas the lithium sublattice (2*a* positions) mainly involves bivalent nickel ions.[108]

It was shown[106] that the concentration-induced order–disorder transition in $Li_{1-x}Ni_{1+x}O_2$ is well simulated by using the 'lattice gas' concept. The dependences of the ordering parameter on the lithium content were obtained, and $\eta_{max} = 0.96$ was found even for the stoichiometric composition. Moreover, it was shown that even the region of the existence of cubic structures ($x \geqslant 0.4$) is characterised by the effects of the short-range structural order, which were studied in detail by synchrotron X-ray emission.[109] Based on the results obtained, the sizes of short-range order domains were assessed.

A small magnitude of the X-ray scattering factor for lithium makes it impossible to determine the degree of cationic disordering in $Li_{1-x}Ni_{1+x}O_2$ near the stoichiometric composition. For this purpose, other methods, such as ESR[110] or X-ray absorption spectroscopy[111] were used. Thus it was found[111] that two different Ni–O distances (2.07 and 1.94 Å) whose ratio varies with *x* are present.

Three successive first-order transitions which occur during electrochemical extraction of lithium[112,113] (at high potentials, completely deintercalated 'NiO_2' phases can also be obtained[114]) cause the following changes in the $LiNiO_2$ structure: hexagonal → monoclinic → hexagonal′ → hexagonal″. The relationships between the unit cell parameters of monoclinic (*C*2*m*, similar to that observed for $NaNiO_2$) and hexagonal phases are as follows:

$$a_m = \sqrt{3}a_h,$$

$$b_m = a_h,$$

$$c_m = \frac{c_h}{3\sin\beta},$$

$$\beta = 180 - \text{arctg}\frac{c_h}{\sqrt{3}a_h}.$$

It is also important that the monoclinic phase is only formed upon deintercalation of virtually stoichiometric $Li_{1-x}NiO_2$, whereas intercalation of $Li_{1-x}NiO_2$ with $x \geqslant 0.05$ does not affect the symmetry.[115] Stoichiometry of the initial compound also affects the process of chemical deintercalation: with a decrease in the lithium content, extraction of lithium and admixed nickel from lithium layers is supplemented by ion exchange which involves protons.[116]

The presence of nickel in the lithium layers plays a significant role in the stabilisation of the monoclinic phase.[117] Using EXAFS methods, it was shown[118] that the local distortion of NiO_6 octahedra in the monoclinic deintercalated phase of Li_xNiO_2 ($0.5 < x < 0.75$) is substantially weaker compared with the stoichiometric trigonal phase. This was attributed to the electron exchange between Ni^{3+} and Ni^{4+} sites. Also, the results of electron-microscopic studies have shown the monoclinic phase to involve a superstructure formed by partially ordered lithium ions (vacancies in the lithium layers).[119] The deintercalated Li_xNiO_2 phase is thermally unstable, and the layered hexagonal structure gives way to the cubic spinel structure at 453 K, which is accompanied by oxygen loss.[120]

Efforts were undertaken to obtain the $Li_{1+x}NiO_2$ oxide superstoichiometric with respect to lithium.[121,122] For instance, a phase with $x \geqslant 0.3$ having a monoclinic structure was described.[122,123] The latter was formed by closely packed oxygen layers (slightly distorted) which separated purely lithium layers from those filled by 1/3 with lithium ions and by 2/3 with nickel ions.

III. Magnetic properties of $LiMO_2$ oxides

Structural differences in the series of $LiMO_2$ oxides, where M is a transition 3*d* metal, are not significant: the crystal structures differ only in the mode in which the cations of alkali and transition metals are ordered in the planes of the parent cubic lattice. Nonetheless, these compounds exhibit fairly diverse magnetic properties.

$LiVO_2$. Magnetic effects which suggest phase transitions in $LiVO_2$ were first described by Bongers.[13] Heating above 450 K results in a fourfold increase in the magnetic susceptibility (Fig. 4); at higher temperatures, the latter is practically independent of the temperature. To explain the magnetic properties of $LiMO_2$ in the region below the transition temperature, a mechanism of formation of molecular orbitals in the basal plane of the hexagonal $LiVO_2$ structure was proposed.[125] The trigonal V_3 clusters thus obtained are nonmagnetic due to Heisenberg antiferromagnetic exchange coupling, and the phase transition is associated with their decomposition.

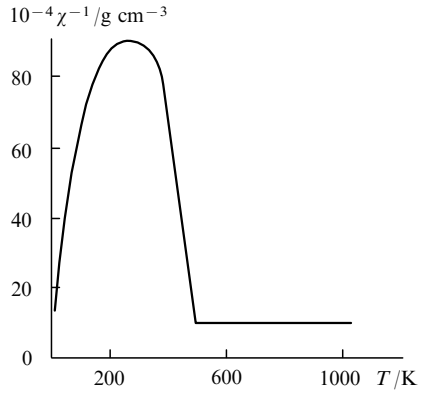


Figure 4. Temperature dependence of the reciprocal magnetic susceptibility of $LiVO_2$.[124]

Another model proposed[4,126] does not imply any changes in the symmetry. This interprets the low-temperature magnetic data in terms of the existence of a two-dimensional 'metal' cluster built by vanadium ions bound by metal–metal bonds. In the high-temperature region, *d* electrons are delocalisated, and $LiVO_2$ becomes a narrow-zone metal. This fact was evidenced by IR spectra, results on electrical conductivity[4] and the data from X-ray absorption spectroscopy.[127] Phase transitions which, as in the above model, were attributed to the changes in the critical M–M distance are typical of many transition-metal simple oxides: V_2O_3, VO_2, V_4O_7, Ti_3O_5, Ti_4O_7.[128–131] The role the structural changes in $LiVO_2$ play in the first-order phase transition from nonmagnetic to magnetic phase was discussed in detail.[132] It has been found that due to the changes in the magnetic energy the high-temperature phase is more stable.

$LiCrO_2$. The studies on the magnetic properties of $LiCrO_2$ as well as of many other oxides were pioneered by Bongers.[13] Magnetic susceptibility data indicated antiferromagnetic ordering to exist below 300 K and the Curie–Weiss paramagnetism with $\Theta = -577$ K and $\mu_{ef} = 3.71$ μ_B to be present above 300 K. These characteristics were refined later: the Néel temperature (T_N) was found to be 56 K[133]; the value of μ_{ef} obtained by ESR technique[134] was 3.8258 μ_B (the deviation from an intrinsic spin value by 0.0529 μ_B was attributed to spin-orbit coupling).

Many studies have been made of the magnetic structure of $LiCrO_2$.[135–137] The structure was assumed[135] to be two-dimensional with an exchange-coupling constant inside the layer of $J = -39 \pm 1$ K. Based on the results of neutron scattering on $LiCrO_2$ single crystals, a magnetic structure with a single propagation vector $\mathbf{k} = [1/3, -2/3, 3/3]$ has been proposed.[137]

The relative orientation of the spins of neighbouring Cr^{3+} ions in the magnetic planes of $LiCrO_2$ was explained by the competition of direct antiferromagnetic interactions and indirect ferromagnetic double exchange coupling.

In many studies (see, *e.g.*, Refs 138, 139), the structure of $LiCrO_2$ was considered as a Heisenberg trigonal lattice. Such compounds attract attention due to the fact that ferromagnetic compounds can involve different magnetic orders compared with the classical Néel order. A joint analysis of the data on susceptibility, neutron scattering and magnetisation have led to the following conclusions:[140] first, during the magnetic phase transition, a 120-degree magnetic structure which involves Cr^{3+} ions is formed in each layer; in the process, the magnetic ordering both in the layers and along the *c* axis occurs at the same Néel temperature; second, the magnetic structure is characterised by two wave vectors $\mathbf{k} = [1/3, 1/3, 0]$ and $[-2/3, 1/3, 1/2]$.

Figure 5 shows the temperature dependence of the magnetic susceptibility of $LiCrO_2$.

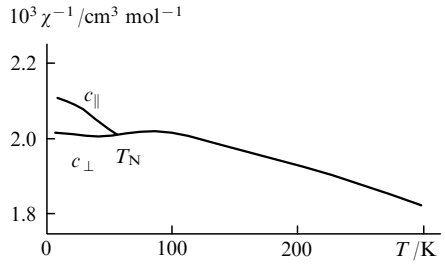


Figure 5. Temperature dependence of the magnetic susceptibility of $LiCrO_2$.[140]

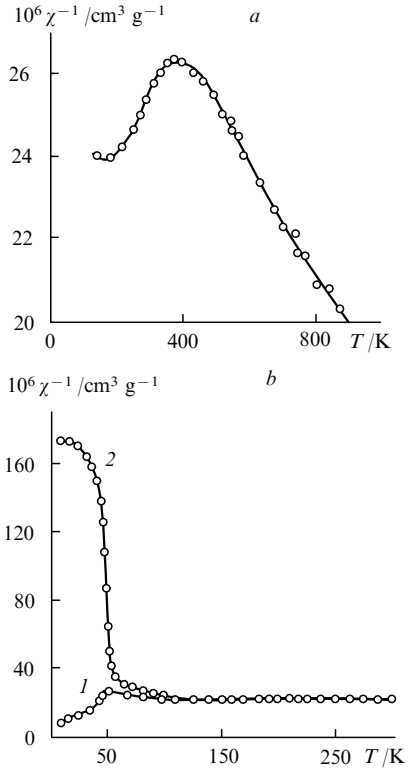


Figure 6. Temperature dependence of the magnetic susceptibility of $LiMnO_2$ in the regions (*a*) 100 – 1000 K and (*b*) 4 – 300 K.[141, 142] (*1*) Cooling in a zero field; (*2*) cooling in a 100-Œ field.

$LiMnO_2$. The first information on the magnetic properties of orthorhombic $LiMnO_2$ can be found in Ref. 13, in which the antiferromagnetic transition at 300 K was deduced. This fact was confirmed by more detailed studies.[39, 141] The magnetic susceptibility variation is characterized by the following features: the paramagnetic behaviour follows the Curie – Weiss law at temperatures above 600 K ($\Theta = -1056$ K, $\mu_{ef} = 4.82\ \mu_B$ per Mn^{3+} ion); the magnetic susceptibility passes a broad maximum at 400 K and its polytherms diverge below 100 K, being measured upon cooling both in the zero field and in the 100-Œ applied field (Fig. 6). Based on the results on neutron scattering, the magnetic structure of $LiMnO_2$ was supposed to have a propagation vector $\mathbf{k} = [1/2, 1/2, 1/2]$ and a magnetic moment equal to 3.69 μ_B per Mn^{3+} ion and preferentially oriented along the *b* axis. The Néel temperature, which characterises a phase with three-dimensional magnetic order, is 261.5 K;[141] above this value, the effects of short-range 2D order are observed.

Yet another magnetic effect observed in $LiMnO_2$ at 50 K was probably the result of weak ferromagnetism.[139, 141] Its magnitude and the temperature of its manifestation depended on the stoichiometry. It was shown [142] that even a small number of structural defects can radically change the magnetic characteristics of $LiMnO_2$ in this region. The magnetic susceptibilities of $Li_{0.99}MnO_2$, $Li_{1.01}MnO_2$ and $LiMnO_{1.99}$ compositions were measured. Presumably, the manganese ions present in lithium sites which serve as the bridges between the double layers of manganese are the most probable reason for the formation of the three-dimensional magnetic structure.[142] This is why $Li_{0.99}MnO_2$ was assumed to be more prone to three-dimensional ordering than $LiMnO_2$. At the same time, the presence of excess lithium in $Li_{1.01}MnO_2$ should apparently hinder the formation of defects of the Mn_{Li} type and, hence, the formation of the three-demensional magnetic structure. The results obtained for defective samples confirmed this assumption: indeed, the appearance of Mn_{Li} defects favoured the formation of the three-dimensional magnetic structure. An analysis of magnetisation curves have shown the spontaneous magnetisation to increase in the sequence $Li_{1.01}MnO_2$, $Li_{0.99}MnO_2$, $LiMnO_{1.99}$ and to be equal to 0.282, 0.333 and 0.421 G cm^3 g^{-1}, respectively. The coercive force increases in the same sequence: 1100, 2651 and 5974 Œ. The fact that the temperature of magnetic ordering is higher for lithium-deficient and oxygen-deficient compositions compared with stoichiometric $LiMnO_2$ also confirms the hypothesis put forward.

A cubic modification of $LiMnO_2$ obtained at high pressure exhibits antiferromagnetic properties with $T_N = 40$ K, $\Theta = -200$ K and $\mu = 4.90\ \mu_B$.[4]

$LiFeO_2$. At low temperatures, all three modifications of $LiFeO_2$ (α, β and γ) are antiferromagnetically ordered (Fig. 7); the Néel temperature is 42 K for α- and β-$LiFeO_2$ and 295 K for γ-$LiFeO_2$. For all three modifications, the temperature dependences of the magnetic susceptibility were shown to deviate in the paramagnetic region from the Curie – Weiss law, which was

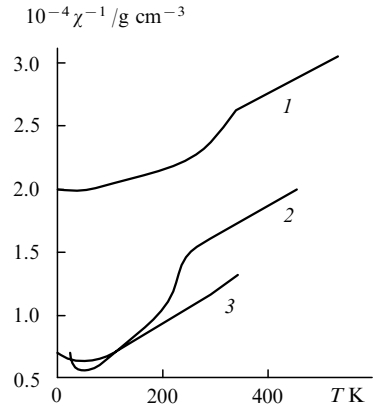


Figure 7. Temperature dependence of the reciprocal magnetic susceptibility of $LiFeO_2$.[57] (*1*) γ- $LiFeO_2$; (*2*) α-$LiFeO_2$: (*3*) β-$LiFeO_2$.

associated with the fact that distributions of iron and lithium ions involve elements of the short-range order. The magnetic structures of α- and γ-$LiFeO_2$ were found [143] in studies on the Mössbauer effect and from the results of neutron scattering. The latter structure is characterised by tetragonal magnetic symmetry with strong antiferromagnetic superexchange coupling of Fe^{3+} ions in (001) planes and much stronger interplane interaction. Magnetic moments of ions are directed along the [001] axis. The magnetic structure of the α-$LiFeO_2$ cubic phase is characterised by ferromagnetically ordered spins inside parallel (111) planes, the latter being antiferromagnetically bound with one another. For this structure to appear, it is necessary that lithium and iron ions are substantially separated in alternate (111) planes. Such a trend was demonstrated by the studies on the Mössbauer effect.

Magnetic properties of a metastable layered modification of $LiFeO_2$ prepared by the hydrothermal method were described.[144, 145] The antiferromagnetic ordering was shown to exist below 20 K. No effects associated with the transition into the spin-glass state typical of the isostructural $LiNiO_2$ phase were observed. It was shown that variations in the degree of cationic ordering affect the Néel temperature.

$LiCoO_2$. Trivalent cobalt in $LiCoO_2$ is in the low-spin state [146] $(t_{2g}^{\alpha})^3 (t_{2g}^{\beta})^3 (e_g)^0$, hence, its magnetic moment is equal to zero. This is why the magnetic susceptibility of $LiCoO_2$ should not depend on the temperature. However, this statement is only true for stoichiometric specimens.[147] The defects present in $LiCoO_{2-x}$ and the attendant paramagnetic centres which are apparently represented by Co^{2+} ions increase the magnetic susceptibility and make it temperature-dependent. This was confirmed by the results of thermogravimetry. The paramagnetic component was also described for $LiCoO_2$ superstoichiometric with respect to lithium.[82]

Above 750 K, the polytherms of magnetic susceptibility of both stoichiometric and defective $LiCoO_2$ were found to ascend reversibly [13, 147] (Fig. 8). Such an increase with the temperature indicated the appearance of paramagnetic centres. The following assumptions on the nature of these centres were drawn.

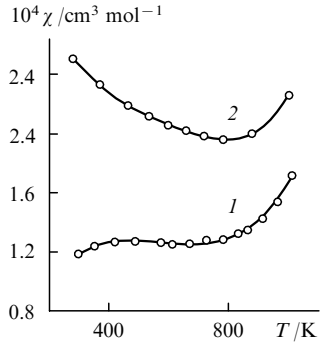


Figure 8. Temperature dependences of the magnetic susceptibility of $LiCoO_2$.[147] (*1*) Synthesis and measurements in an oxygen atmosphere; (*2*) synthesis and measurements under reduced pressure.

1. At temperatures above 750 K, thermally activated centres appear in $LiCoO_2$ as a result of oxygen exchange with the gas phase. The following process of defect formation is possible, which results in the formation of paramagnetic centres Co^{2+} (Co'_{Co}):

$$2Co_{Co} + O_O \longrightarrow (1/2)\,O_2(g) + V_O^{\cdot\cdot} + 2Co'_{Co}\,.$$

The appearance of each oxygen vacancy leads to the formation of two paramagnetic centres.[147]

2. The reason for the increase in the magnetic susceptibility is the transition of Co^{3+} ions to the high-spin state $(t_{2g}^{\alpha})^3 (t_{2g}^{\beta})^1 (e_g)^2$ ($\mu_{ef}^2 = 24\ \mu_B^2$).[13]

The magnetic susceptibility of chemically delithiated $LiCoO_2$ was studied.[92] This was shown to obey the Curie–Weiss law in the temperature interval from 83 to 300 K for all compositions irrespective of the degree of lithium extraction. The values of the effective moment were as follows:

Oxide	$LiCoO_2$	$Li_{0.92}CoO_2$	$Li_{0.76}CoO_2$	$Li_{0.61}CoO_2$
μ_{ef}/μ_B	1.157	1.164	1.731	1.733

The effective magnetic moments of the latter two compositions almost coincided. This was associated with changes in the degree of electron localisation.

$LiNiO_2$. The magnetic properties of layered $LiNiO_2$ depend on both the stoichiometry and the degree of structural order. The results of numerous experiments were often conflicting. This also concerns the manifold interpretations of the data obtained.

Thus it was concluded [96] that magnetic properties of $LiNiO_2$ can adequately be described on an assumption that trivalent nickel ions are in the low-spin state $[(t_{2g}^{\alpha})^3 (t_{2g}^{\beta})^3 (e_g)^1]$. Later, this fact has found an experimental confirmation [148] and was substantiated theoretically.[149] However, in a number of studies (*e.g.*, in Ref. 150), trivalent nickel is assumed to be in the high-spin state $[(t_{2g}^{\alpha})^3 (t_{2g}^{\beta})^2 (e_g)^2]$, which forms a Kramers doublet with $S = 1/2$.

A different viewpoint exists: the magnetic properties of $LiNiO_2$ are determined by the exchange-coupled ($Ni^{2+} - O^{1-}$) pairs.[151] Charge-compensation processes in $LiNiO_2$, which are responsible for the appearance of holes in the oxygen zone, resemble those observed in high-temperature superconductors and were revealed for the first time in the studies of X-ray absorption spectra for the $Li_xNi_{1-x}O$ system.[151] Similar results were obtained in other studies.[152, 153] Calculations [154] confirmed that an electron hole appears in the 2*p* oxygen band rather than in the 3*d* nickel band. However, the fact that such techniques as ^{7}Li NMR and ESR [155] have not confirmed this observation deserves mention.

In a number of studies, the magnetic properties of $LiNiO_2$ were considered in relation to the problem of the ground state of a two-dimensional (2D) triangular lattice antiferromagnet with $S = 1/2$. Thus within the framework of the model of a quantum liquid (resonance valence zone), it was assumed for the first time [156] that the ground state of such systems in the absence of long-range magnetic order has a low energy compared with the classical Néel state. This problem was the subject of wide speculation in the context of the assumption that it is the resonance valence zone that is responsible for high-temperature superconduction in copper complex oxides.[157] The $LiNiO_2$ oxide characterised by $S = 1/2$ and a structure based on face-centred cubic packing of oxygen atoms where nickel and lithium atoms occupy the interstices and form alternate layers (as a result, the interlayer distances substantially exceed those between magnetic atoms inside a layer) can well be described by the aforementioned model.[150, 155, 158, 159]

The magnetic properties of a number of $Li_xNi_{1-x}O$ solid solutions and $LiNiO_2$ as the end member of this series were studied in detail.[96] The main attention was focused on the magnetic transition in the temperature range of 200–300 K (this temperature is usually denoted as T_{N1}), which was claimed to be of the ferromagnetic nature. The dependences of the Curie temperature and magnetisation of $Li_xNi_{1-x}O$ on concentration had maxima at $x = 0.43$ (Fig. 9), and the degree of structural order η [the degree of cationic ordering in (111) alternate planes of the basal NaCl lattice] increased monotonically with an increase in the lithium content and reached a maximum for $LiNiO_2$, which, however, was below 100%. It is the latter observation that explained the fact that magnetic measurements carried out later [97, 98, 160–162] for $LiNiO_2$ samples with a higher degree of structural ordering revealed no magnetic transition described in Ref. 96. Thus, the magnetic ordering is an indicator of $\eta < 1$. The fact that the magnetic properties of $LiNiO_2$ can indicate the structural ordering of a sample stems from the structural peculiarity of perfectly ordered $LiNiO_2$ [namely, the fact that each plane occupied by

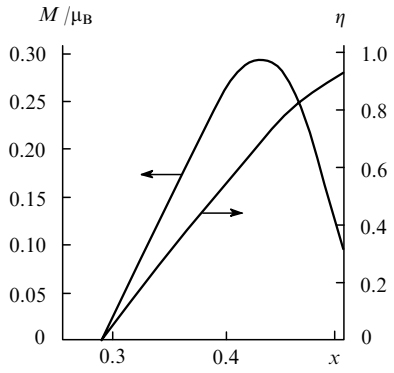


Figure 9. Concentration dependences of magnetisation M and degree of ordering η in $Li_xNi_{1-x}O$.[96]

magnetic ions (Ni^{3+}) is separated from another plane by three nonmagnetic planes (O–Li–O)] and the partial disordering caused by the presence of nickel ions in lithium sites (and *vice versa*).

A complete cationic disordering ($\eta = 0$) is typical of cubic $LiNiO_2$ the magnetic properties of which have been described.[98] The polytherm of its magnetic susceptibility demonstrated an anomalous feature, which allowed the paramagnetic—antiferromagnetic transition at 280 K to be deduced (Fig. 10).

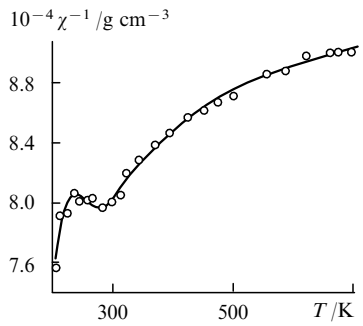


Figure 10. Temperature dependence of the reciprocal magnetic susceptibility of $LiNiO_2$ with the degree of ordering $\eta = 0$.[98]

The magnetic transition occurring in this oxide at 210 K was studied in detail [150, 158, 159]. The magnetic structure of $LiNiO_2$ was simulated on an assumption of a perfect ordering. However, from the synthetic conditions mentioned ($LiOH + Ni_2O_3$; $T = 1100$ K) suggest that the degree of ordering in the samples studied did not exceed $\eta = 0.8$. Below the transition temperature, $LiNiO_2$ was found to exhibit the ferrimagnetic behaviour. However, in contrast to classical ferrimagnetic materials, the field dependence of the magnetisation [$M(H)$] in $LiNiO_2$ was nonlinear below T_{N1}, did not reach saturation and infinitely increased with the field strength according to $M \propto H^{1/\delta}$.

It should be noted that the possibility of assigning the magnetic transition which occurs in $LiNiO_2$ with $\eta < 1$ in the temperature interval of 150–300 K to the ferrimagnetic type [96] was not confirmed later. In neutron diffraction studies,[150, 163] magnetic reflexes were not observed below the transition point even on long-term exposures. The ordering at 240 K was found [161] to be of a ferromagnetic nature. The same conclusion was made in Ref. 98.

In addition to the magnetic transition observed in the region of 150–300 K, the temperature and even the possibility of which depend on the degree of the structural order of $LiNiO_2$, other anomalous magnetic features were observed at lower temperatures. A broad spectrum of mechanisms were invoked for their

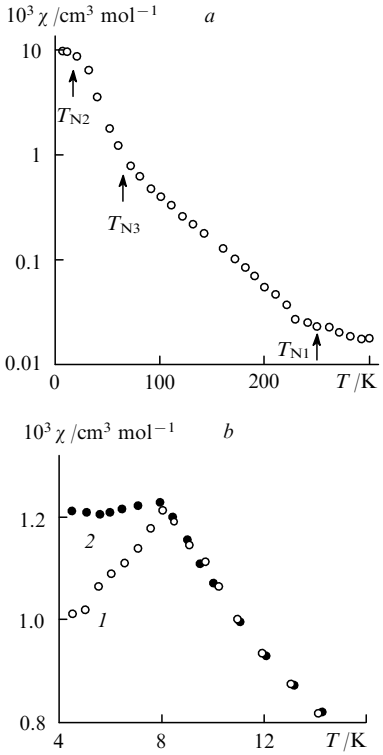


Figure 11. Temperature dependences of the magnetic susceptibility of $LiNiO_2$ measured in an applied field of (*a*) 1000 [165] and (*b*) 10 Œ.[162] (*1*) Cooling in a zero field; (*2*) cooling in a 10-Œ field.

explanation. For example, virtually stoichiometric and perfectly ordered $LiNiO_2$ with Ni–Ni interactions of the 2D type was shown [160, 162, 164] to behave as a typical spin glass. The temperature dependence of the magnetisation measured upon zero-field cooling demonstrated a sharp peak at 9 K (this temperature was denoted as T_{N2}; according to the results of other authors, T_{N2} is 35–50 K, see, *e.g.*, Ref. 165). At the same time, upon cooling in a nonzero field, the magnetic susceptibility increased monotonically (Fig. 11). The frequency dependence of the height and position of the peak, which was obtained by measuring the AC susceptibility, also indicated the attainment of a spin glass state. In certain studies,[159, 166] the state below T_{N2} was considered as the quantum liquid state in which the spins form mobile pairs. The temperature $T_{N2} = 6$ K was claimed [161] to be the Curie temperature for a two-dimensional Ising system. Such a conclusion was drawn by taking into account the fact that the slope of the linear dependence $\ln(M/H)$ *vs.* $\ln(T-T_c)$ was found to be equal to -1.7, which agrees with the critical factor of $-7/4$ for the 2D model of Ising.[167]

The temperature dependence of the magnetic susceptibility of $LiNiO_2$ demonstrated yet another special point in the temperature range from 70 to 80 K, *viz.*, T_{N3}.[165] The values of both T_{N2} and T_{N3} depended on the sample quality.[165] The magnetic behaviour of $LiNiO_2$ at low temperatures can be described as follows.[164]

1. The $T_{N3} < T < T_{N1}$ interval corresponds to nonlinear magnetisation in the external field. The magnetic entropy decreases by 20%. A model of the spin-system inhibition for the antiferromagnetic triangular lattice with the planar short-range order is realised.

2. In the $T_{N2} < T < T_{N3}$ region, magnetisation sharply increases. The magnetic entropy decreases twofold in the absence of any noticeable anomalies which would have indicated the appearance of a long-range magnetic order. The interactions between the layers are assumed to generate the effects of the three-dimensional short-range order.

3. In the $T < T_{N2}$ region, the temperature dependence of the magnetisation tends to saturation. A noticeable residual magnetic

entropy is preserved up to T_{N2}. No anomalies associated with the long-range order are observed. The existence of a frozen spin state somewhat different from that of common spin glasses is assumed. The difference lies in the fact that the temperature dependence of the specific heat is quadratic in the former case and linear in the latter case.

Due to a strong 180-degree aniferromagnetic $Ni_{Li}-O-Ni_{Ni}$ interaction, a ferromagnetic coupling of nickel ions located above and below the Li layer arises, and a small ferromagnetic cluster forms around the Ni_{Li} defect.[168] The existence of such a cluster was proved experimentally by ESR in an applied field of up to 245 GHz.[169] Two types of clusters were observed: those of the first type are formed below 235 K, the other are formed below 120 K. Such a system was proposed to be considered as a superparamagnetic one, *i.e.*, built of separate ferromagnetic domains.[155] The formation of the latter is consistent with the fact that spontaneous magnetisation is suppressed in layered oxides.[170]

Above the temperature of magnetic ordering, the magnetic susceptibility of $LiNiO_2$ is adequately described by the Curie–Weiss law the parameters of which found by different authors differ substantially [μ_{ef} = 1.84 μ_B, Θ = 79.3 K (see Ref. 164); μ_{ef} = 2.2 μ_B, Θ = 2 K (see Ref. 171)]. These parameters also depended on the stoichiometry and the degree of structural order. The temperature dependence of $1/\chi$ in the magnetically disordered region was not smooth and consisted of linear segments.[98] Taking this into account, it was assumed that yet another phase transition takes place in $LiNiO_2$, *viz.*, a paramagnetic–paramagnetic transition. A possible reason for the break observed in $1/\chi$ *vs.* T dependences is the transition of nickel from the low-spin to high-spin state. Table 1 lists the parameters of the Curie–Weiss equation determined for the low-temperature and high-temperature segments of the $1/\chi$ *vs.* T dependences for $LiNiO_2$ samples with different η values. It is noteworthy that the magnetic moments and the Weiss constants of two paramagnetic phases approach one another with an increase in the degree of structural ordering. It appears that these parameters can serve as indicators of the completeness of the cationic ordering in $LiNiO_2$.

Table 1. Magnetic moments and Weiss constants of $LiNiO_2$ with different degrees of structural ordering.[98]

η	T = 200–400 K		T = 600–900 K	
	μ_{ef}/μ_B	Θ /K	μ_{ef}/μ_B	Θ /K
0.67	1.489	185	2.547	−287
0.85	1.751	131	2.201	−87
0.94	1.869	31	2.061	−36
0.98	1.987	33	2.237	−20

It is interesting that $LiNiO_2$, which was shown to be antiferromagnetically ordered in its metastable structurally disordered state and ferromagnetically ordered at sufficiently high degrees of structural ordering [η = 0.6–0.8 (see Ref. 98)], retained its paramagnetic properties up to the liquid helium temperature for the case of perfect ordering. The latter observation can be explained by the fact that, as was shown by de Jongh and Miedema,[172] two-dimensional Heisenberg systems which apparently involve the perfectly ordered $LiNiO_2$ oxide [98] have no long-range magnetic order. The experimentally observed phase transitions in these systems were caused by deviations from the ideal behaviour, which resulted in an interaction arising between the layers. For example, $(C_nH_{2n+1}NH_3)Cu_4Cl_2$ (see Ref. 173) with a small number of nonmagnetic layers separating the magnetic layers has ferromagnetic properties, while the same substance with a greater number of nonmagnetic layers exhibits no ferromagnetism. For $LiNiO_2$, it is those nickel ions which occur in the lithium layers due to partial disordering that are responsible for the interlayer interaction.

In view of the fact that the degree of structural order in $LiNiO_2$ is closely related to stoichiometry, the magnetic properties depend even on small changes in x in $Li_{1-x}Ni_{1+x}O_2$. This was confirmed in a study [160] in which it was shown that samples with $x \leqslant 0.01$ demonstrate a thermomagnetic hysteresis typical of a spin glass at 8 K, whereas samples with $x \approx 0.08$ exhibit spontaneous magnetisation at 5 K, which corresponds to a magnetic moment of ~ 0.3 μ_B/Ni. Similar results were obtained in another study [174]: it was observed that $LiNiO_2$ is a spin glass, in contrast to $Li_{0.93}Ni_{1.07}O_2$.

IV. Structure and magnetic properties of $LiM_{1-x}M'_xO_2$ solid solutions

The $LiMO_2$ oxides under consideration can form solid solutions. The attention paid to solid solutions, first of all, is associated with the prospects of stabilising the structural types which can be used as cathodic materials in electrochemical devices. Moreover, solid solutions formed by compounds with different types of cationic ordering are interesting from the viewpoint of studying the short-range order effect, the three-dimensional–two-dimensional structural transitions and the formation of new superstructures.

$LiNi_{1-x}Co_xO_2$ ($0 \leqslant x \leqslant 1$). Oxides $LiNiO_2$ and $LiCoO_2$ form a continuous series of solid solutions, which, like the original phases, have a trigonal structure with the $R\bar{3}m$ symmetry. With a decrease in the content of cobalt (the ionic radius of which is smaller than that of nickel), the cell parameters a and c decrease monotonically. However, the concentration dependence of the c/a ratio is not monotonic, and for x = 0.3 its slope changes, *i.e.*, the increase in the c/a ratio slows down.[175] This result was reproduced in another study;[176] however, the authors of the latter study have attributed the singular point to the composition with x = 0.5. In their opinion, an increase in c/a from 4.96 (x = 0.5) to 4.99 (x = 1) does not bring about mixing of lithium and nickel ions in the octahedral positions of the hexagonal face-centred lattice. The value c/a = 4.99 corresponds to a perfect hexagonal unit cell. For smaller c/a values and hence for higher nickel concentrations, partial cationic disordering takes place, which results in a deviation of the $LiNi_{1-x}Co_xO_2$ symmetry from the ideal hexagonal towards the parent cubic one. For a perfect close-packed structure of the $Fm\bar{3}m$ symmetry, c/a = 4.90. Based on the results of X-ray diffraction analysis (the Rietveld method), it was found [177] that, at low cobalt contents ($x \leqslant 0.2$), the excessive bivalent nickel ions are always present in solid solutions studied: $Li_{1-z}Ni_{1+z-t}Co_tO_2$ [$t = x(1 + z)$]. An increase in the cobalt content reduces the nonstoichiometry and stabilises the 2D structure.

The stabilising effect cobalt has on the 2D structure of the solid solution also manifests itself in electrochemical intercalation. Phase transitions that take place during electrochemical intercalation of $LiNiO_2$ do not occur in solid solutions.[178] This is explained by the fact that cobalt suppresses the ordering of lithium vacancies. At the same time, it is noteworthy that deep chemical extraction of lithium from solid solutions enriched with nickel results in a monoclinic distortion of the lattice.[179]

To avoid the distortion of the regular layered structure (2D) of $LiNi_{1-x}Co_xO_2$ solid solutions, the low-temperature synthetic methods were applied, using, *e.g.*, β-$Ni_{1-y}Co_yOOH$ [180] or $Ni_{1-y}Co_y(OH)_2$[181] as the starting materials. Solid solutions with minimum cationic disordering were obtained by the sol–gel method [182, 183] (this also refers to pure $LiNiO_2$), pyrolysis [184] and co-precipitation from solutions.[185]

^{6}Li and ^{7}Li NMR studies on $LiNi_{1-x}Co_xO_2$ solid solutions ($0 \leqslant x \leqslant 1$) carried out in both static and dynamic modes [186, 187] have revealed structural microheterogeneities unrelated to the cationic ordering. These microheterogeneities did not cause any phase formation and could not be revealed by the diffraction techniques. They represented clusters of several cobalt atoms.

A magnetic phase diagram (Fig. 12) was constructed based on the results of detailed studies of magnetic properties of $LiNi_{1-x}Co_xO_2$ solid solutions ($0 \leqslant x \leqslant 1$).[188] A model was pro-

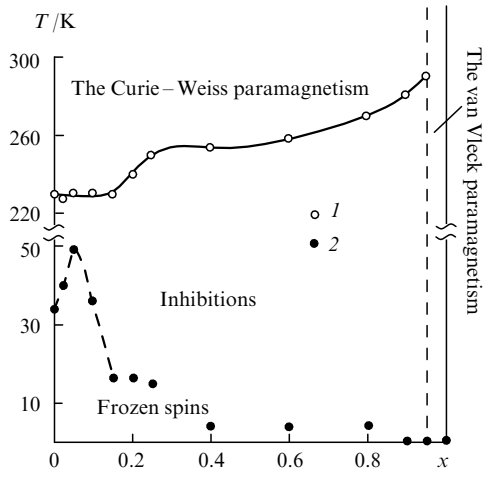


Figure 12. Magnetic phase diagram of $LiNiO_2-LiCoO_2$ system.[188] (*1*) T_{N1}; (*2*) T_{N2}.

posed that described the magnetic properties of both $LiNiO_2$ and $LiNi_{1-x}Co_xO_2$. This model is based on an assumption of an antiferromagnetic interaction within a layer and a weak ferromagnetic bonding between the layers. A conclusion that a system of three sublattices is unstable which was drawn from this model is of prime importance. It is with this conclusion that the absence of magnetic reflexes (1/3 1/3 *n*) is related.

The data on $LiNi_{1-x}Co_xO_2$ solid solutions additionally doped with manganese,[189] magnesium [190] and strontium [191] can be found in the literature.

$LiNi_{1-x}Ti_xO_2$ ($0 \leqslant x \leqslant 0.5$). According to the results of X-ray analysis,[192] the solid solutions with $0 \leqslant x \leqslant 0.3$ are isostructural to the layered $LiNiO_2$. At a higher titanium content, the structure becomes cubic, due to complete cationic disordering. The structural data refined using the Rietveld technique indicated that $LiNi_{0.7}Ti_{0.3}O_2$ also involves a certain number of transition metal ions in the lithium layers; hence, the regular two-dimensional structure is distorted. It is of note that these layers involve bivalent nickel and trivalent titanium. This result was obtained by means of the XPS technique. The authors of this study [192] did not mention the mechanism of the charge compensation in $LiNi_{0.7}Ti_{0.3}O_2$ solid solutions which involve Ni^{2+} ions: whether a certain number of titanium ions appears or the oxygen content changes. It should be noted that the degee of oxidation of Ti (Ti^{3+}) is not typical of titanium compounds synthesised in air at sufficiently high temperatures, *i.e.*, under conditions in which the solid solutions under discussion have been prepared.

$LiNi_{1-x}Mn_xO_2$. Solid solutions isostructural to $LiNiO_2$ were studied.[193–199] Certain cationic disordering was described [197] within the frameworks of the hexagonal structure and later confirmed.[193] To stabilise the trivalent state of nickel ions and thereby stabilise the layered structure, a special procedure of coprecipitation in an oxidative medium was developed.[193] As a result, solid solutions with the composition $LiNi_{1-x}Mn_xO_{2+\delta}$ ($0 \leqslant x \leqslant 0.5$) were obtained. The oxidation states of the transition metals in these solid solutions were determined by measuring the magnetic susceptibilities. It was shown that both transition metals in the sample bulk are in the trivalent state, whereas traces of Mn^{4+} were detected on the surface. All solid solutions studied exhibited a ferromagnetic transition at a temperature (T_C) which increased with the manganese content. The exception was pure $LiNiO_2$, which is characterised by a strong interlayer ferromagnetic interaction of the Ni(3*b*)–O–Ni(3*a*)–O–Ni(3*b*) type responsible for the high T_C. The existence of the ferromagnetic transition both in pure $LiNiO_2$ and $LiNi_{1-x}Mn_xO_{2+\delta}$ solid solutions points to the incomplete cationic ordering and to the presence of transition metal ions in the lithium layers. Table 2 shows the magnetic characteristics of $LiNi_{1-x}Mn_xO_{2+\delta}$ ($0 \leqslant x \leqslant 0.5$).

Table 2. Magnetic characteristics of $LiNi_{1-x}Mn_xO_{2+\delta}$ ($0 \leqslant x \leqslant 0.5$).[193]

x	Θ /K	μ_{ef}/μ_B		T_C /K
		experiment	calculation	
0	162	1.7	1.74	196
0.1	−118	2.1	2.06	39
0.2	−55	2.2	2.37	53
0.4	−96	3.0	3.00	72
0.5	−107	3.3	3.32	88

$LiNi_{1-x}Fe_xO_2$. The $LiNi_{1-x}Fe_xO_2$ system demonstrates two types of solid solution. Compositions with $0 < x < 0.22$ are isostructural to $LiNiO_2$. Their degree of ordering gradually decreases, which manifests itself in weaker X-ray reflections superstructural to those of the sodium chloride cubic lattice. Moreover, cubic solid solutions are formed in the concentration interval of $0.42 < x < 1$. In the intermediate region, two phases are present.[200–202] By studying this systems, one can follow the changes in the magnetic properties that occur with a decrease in the dimensionality from 3D ($LiFeO_2$) to 2D ($LiNiO_2$).

At $T > 300$ K, the magnetic susceptibilities of all $LiNi_{1-x}Fe_xO_2$ compositions obey the Curie–Weiss law. The first group of solid solutions is characterised by a transition to a magnetically ordered phase. The transition temperature and spontaneous magnetisation both increase with the iron content. The presence of magnetic ordering in the interval from 150 to 200 K points to partial cationic disordering, *i.e.*, the presence of a certain amount of transition metal ions in the Li layers. These results were confirmed by crystallographic data.[203] For a composition with 20% iron, the distribution of cations over positions is: $[Li_{0.965}M_{0.035}]_{3b}[M_{0.965}Li_{0.035}]_{3a}O_2$, M = 0.2Fe + 0.8Ni.

The fact that X-ray patterns of the second group of solid solutions involve no lines superstructural with respect to the NaCl lattice unambiguously indicates that the ions of alkali and transition metals are not ordered in the planes, in contrast to $LiNiO_2$. Nonetheless, at $T < 200$ K, the magnetic susceptibility of this solid-solution group depends on the field strength. This dependence becomes more pronounced with an increase in the nickel content, which points to a magnetic ordering.[201] The magnetisation polytherms statistically processed using the technique of thermodynamic coefficients have revealed no spontaneous magnetisation. Hence, the nonlinear variation of magnetisation for structurally disordered samples is a result of the short-range order associated with the trend of nickel ions for aggregation within the framework of this structure. In other words, the exchange couplings, which are the reason for the magnetic ordering, are limited in solid solutions by certain atomic ensembles. In this case, the condition for percolation do not arise. Such a system is considered [201] as a superparamagnetic one. Based on the concepts mentioned, the cluster size was estimated. The volume of magnetic clusters increased with the nickel content in the cubic solid solution phase, and, at a nickel concentration above 43%, the system first became two-phase and then a hexagonal one.

The number of atoms in clusters (*n*) and the mean size (*d*) of the latter for the superparamagnetic region of $LiFe_{1-x}Ni_xO_2$ are as follows:[201]

x	0.1	0.2	0.3	0.4
n	17	28	38	116
d /Å	7	8	9	13

$LiMn_{1-x}Co_xO_2$ ($0 \leqslant x \leqslant 1$). This group of solid solutions was studied by two groups of researchers.[204, 205] The lattice type was found to be determined by the ratio of transition metal

ions;[205] for $x < 0.2$, oxides with trigonal structures are formed, for $0.2 \leqslant x \leqslant 0.7$, cubic structures are realised and, for higher manganese contents, the symmetry of solutions is tetragonal ($I4_1/amd$). It should be noted that, to obtain solid solutions in the $0.2 \leqslant x \leqslant 1$ concentration interval, the synthesis was carried out in a nitrogen atmosphere.

A different way [205] was chosen for synthesising solid solutions of two layered compounds, *viz*., $LiCoO_2$ and Li_2MnO_3. It was shown that in order to prepare a solid solution (rather than a mechanical mixture of the extreme members), the synthesis should be carried out with an excess of lithium. All solid solutions thus obtained had monoclinic structures. The transformation of a trigonal (hexagonal) unit cell of $LiCoO_2$ into a monoclinic one is expressed as follows (for parameter a as an example):

$$a_h = \frac{1}{\sqrt{3}} a_m .$$

The magnetic properties of $LiMn_{1-x}Co_xO_2$ solid solutions ($0 \leqslant x \leqslant 1$) formed by diamagnetic $LiCoO_2$ and antiferromagnetic $LiMnO_2$ [$T_N = 50$ K, $\Theta = -33$ K, $\mu_{ef} = 3.83\ \mu_B$ (see Ref. 206)] change nonmonotonically: the compounds are paramagnetic for $x \leqslant 0.5$ and the antiferromagnetic transition is observed for higher manganese content. The analysis of the concentration dependence of the effective magnetic moment showed that the oxidation state of manganese is Mn^{4+} for the manganese content > 75%, whereas for its content < 75% the presence of trivalent manganese ions may be assumed.

Methods for the synthesis of $LiMn_{1-x}Co_xO_2$ solid solutions and of $LiMn_{1-x}Ni_xO_2$ and $LiMn_{1-x}Fe_xO_2$ solid solutions with layered structures have been discussed.[207]

$LiCr_{1-x}Fe_xO_2$. This system was studied for both polycrystalline specimens and single crystals.[208] Like $LiNi_{1-x}Fe_xO_2$, this system is formed by two phases, one of which has an ordered layered structure and another has a cubic lattice characterised by a random distribution of metal ions over the lattice positions. It was found that the transition from the cubic structure to trigonal one corresponds to the solution with 73% $LiFeO_2$. A somewhat different value ($\sim 85\%$) was found in another study.[209] The magnetic susceptibility of structurally ordered compositions was shown to have anomalies in the vicinity of 50 K. These anomalies seem to indicate the three-dimensional order. Above the mentioned temperature, the magnetic interactions corresponded to two-dimensional interactions. An analysis of the Mössbauer spectra has shown [210] that 2D interactions also play the key role at low temperatures. At temperatures above 400–600 K, the variation of the magnetic susceptibility obeys the Curie–Weiss law. Table 3 shows the magnetic characteristics of the system. Divergence between experimental and calculated values of the magnetic moment was attributed to anisotropy of magnetic interactions.

In order to explain the parabolic shape of the dependence of the Weiss constant (Θ) on the concentration, the exchange-coupling parameters were separated and the intra- (J_1) and interlayer (J_2) exchange-coupling constants were estimated based on the data from the magnetic susceptibility). In addition, the partial values of the Weiss constants related to different types of coupling were obtained. Thus for interlayer interactions, $\Theta_2^{Cr-Cr} = -185$ K, $\Theta_2^{Cr-Fe} = 59$ K and $\Theta_2^{Fe-Fe} = -30$ K.

$LiV_{1-x}Mg_xO_2$ and **$LiV_{1-x}Al_xO_2$**. These systems were synthesised and studied [211] with the aim of following how the partial substitution of vanadium for an ion with a spin $S \neq 1$ in $LiVO_2$ affects the structural and magnetic parameters of the phase transition. It was assumed that the first system involves V^{2+} ions with $S = 3/2$ and the second system involves Al^{3+} with $S = 0$; the solid solutions have sufficiently narrow homogeneity regions, *viz*., $0 \leqslant x \leqslant 0.06$ and $0 \leqslant x \leqslant 0.1$, respectively. In both systems, the phase transition temperatures were lower than those of pure $LiVO_2$. Moreover, a weak but systematic decrease in the Curie constant was observed in the low-temperature region, which indicated that 'triangular' clusters $V^{3+}-V^{2+}-V^{3+}$ with $S = 1/2$ separated by singlet trimers contributed to the overall susceptibility. Based on these studies, it was concluded that the exchange-coupling constant of V^{3+} ions and the transition temperature both depend on the V–V distance and on the shift of vanadium ions from their positions.

Other solid solutions. Information on $LiAl_xNi_{1-x}O_2$ solid solutions ($x \leqslant 0.25$) with the $LiNiO_2$ structure is availiable.[212, 213] With an increase in the aluminium content, the c/a ratio somewhat increases. It is noteworthy that introduction of aluminium in $LiMO_2$ compounds is considered as one of the factors that stabilise the α-$NaFeO_2$-type layered structure, the latter being the most suitable from the electrochemical viewpoint. Calculations of miscibility carried out for eight compositions of the $LiAl_{1-x}M_xO_2$ system have shown [214] that for M = Ti, V, Cr and Mn layered solid solutions are formed at the temperatures of the conventional synthesis. For M = Fe, Co, Ni and Cu, a low temperature region of immiscibility exists. Special attention was given to $LiAl_{1-x}Co_xO_2$ and $LiAl_{1-x}Cr_xO_2$ systems, which, according to calculations, were completely miscible up to 600 °C. Limitations that arose at higher temperatures were associated with the transition of $LiAlO_2$ into a tetragonal γ-modification.[215] It was experimentally shown [216] that the synthesis carried out at 650 K results in an amorphous modification, whereas at 700–900 K a layered hexagonal structure is formed. It is essential that in $LiAl_{1-x}Co_xO_2$ as well as in $LiAl_{1-x}Ni_xO_2$ aluminium can be shifted from octahedral positions.[217] Synthesis of $LiAl_{1-x}Cr_xO_2$ solid solutions ($0 \leqslant x \leqslant 1$) was described.[218]

Solubility of aluminium in $LiMnO_2$ reached a maximum (5%–7%) at 1220 K.[219] As in the previous case, the existence of the maximum was explained by the formation of γ-$LiAlO_2$. Introduction of even minor amounts of aluminium to $LiMnO_2$ gives rise to a layered structure of the $NaFeO_2$ type. The use of chromium as the dopant led to a similar result.[220]

In addition, the possibility of formation of $LiCr_{1-x}Co_xO_2$, $LiCr_{1-x}Ni_xO_2$,[221] $LiFe_{1-x}Co_xO_2$ [222] and $LiNi_{1-x}B_xO_2$ [223] solutions was demonstrated.

Table 3. Magnetic characteristics of $LiCr_{1-x}Fe_xO_2$.[210]

x	The Curie constant /cm^3 K mol^{-1}	μ_{ef}/μ_B		Θ /K	Θ_1 /K	Θ_2 /K	T_N /K	J_1/k /K	J_2/k /K
		experiment	calculation						
0	1.58	3.57	3.87	−570	−472	−98	15	−33	−6.9
0.1	1.98	4.17	4.07	−546	−399	−147	56	−25	−8.5
0.2	1.76	3.77	4.28	−300	−180	−120	40	−17	−4.3
0.3	1.90	3.91	4.49	−204	−138	−66	35	−11	−2.2
0.4	1.81	3.83	4.69	−25	7.5	−32.5	50	−0.70	−1.1
0.5	1.82	3.83	4.90	0	16.3	−16.3	55	0.58	−0.6
0.6	2.40	4.39	5.10	−47	−35.5	−11.5	45	−1.8	−0.7
0.7	2.64	4.65	5.30	−94	−80.5	−13	40	−3.7	−0.6

V. Conclusion

Complex oxides with the general formula $LiMO_2$ where M is a trivalent transition 3*d* metal are considered as inorganic functional materials of a new generation.[224,225] First of all, this is associated with their good electrochemical characteristics. This factor has stimulated numerous studies not only in applied but also in fundamental directions. Of prime importance are structural and magnetic studies, because the layered structure characteristic of many $LiMO_2$ compounds not only provides adequate diffusion of the alkali metal atoms, which is essential for electrochemical processes, but also is of special interest from the viewpoint of studying low-dimensional magnetic interactions.

At present, the crystal structure of $LiMO_2$ is sufficiently thoroughly described for all stable modifications, and efforts are mainly concentrated on the synthesis and structural description of metastable phases preferentially with layered structures of the α-$NaFeO_2$ type.

The results of investigations of the magnetic properties of $LiMO_2$ show that structural defects may often play the key role in the formation of magnetic structures. First of all, this refers to compounds with variable degrees of structural order.

References

1. R B Goldner, F O Arntz, G Berera, T E Haas, G Wei, K K Wong, P C Yu *Solid State Ion.* **53–56** 617 (1992)
2. S Megahed, W Ebner *J. Power Sources* **54** 155 (1995)
3. C Delmas, in *Industrial Chemistry Library. Lithium Batteries. New Materials, Developments and Perspectives* Vol. 5 (Ed. G Pistoia) (Amsterdam; London; New York; Tokyo: Elsevier, 1994) p. 457
4. T A Hewston, B L Chamberland *J. Phys. Chem. Solids* **48** 97 (1987)
5. R Alcantara, P Lavela, J L Tirado, E Zhecheva, R Stoyanova *J. Solid State Electrochem.* **3** 121 (1999)
6. E J Wu, P D Teresch, G Ceder *Philos. Mag. B* **77** 1039 (1998)
7. R Hoppe *Angew. Chem.* **71** 457 (1959)
8. C J M Rooymans *Z. Anorg. Allg. Chem.* **313** 324 (1961)
9. R Hoppe, B Schepers, H Rohrbon, E Vielhaber *Z. Anorg. Allg. Chem.* **339** 130 (1965)
10. T Birchall, A F Reid *J. Solid State. Chem.* **6** 411 (1973)
11. B L Dickson, K K P Srivastava *J. Solid State Chem.* **19** 117 (1976)
12. Y B Kuo, W Scheld, R Hoppe *Z. Kristallogr.* **164** 121 (1983)
13. P F Bongers Ph D Thesis, The University of Leiden, Leiden, 1957
14. A Lecerf *Ann. Chim., Sci. Mater.* **7** 513 (1962)
15. D W Murphy, M Greenblatt, S M Zahurak, R J Cava, J V Waszczak, G W Hull, R S.Hutton. *Rev. Chim. Miner.* **19** 442 (1982)
16. R J Cava, D W Murphy, S Zahurak, A Santoro, R S Roth *J. Solid State Chem.* **53** 64 (1984)
17. A F Wells *Structural Inorganic Chemistry* (Oxford: Clarendon Press, 1984)
18. T A Hewston Ph D Thesis, The University of Connecticut, Storrs, CT, 1985
19. W Rüdorff, H Becker *Z. Naturforsh., B Chem. Sci.* **9** 613 (1954)
20. B Reuter, R Weber, J Jaskowski *Z. Electrochem.* **66** 832 (1962)
21. K Kobayashi, K Kosuge, S Kachi *Mater. Res. Bull.* **4** 95 (1969)
22. T A Hewston, B L Chamberland *J. Solid State Chem.* **65** 100 (1986)
23. L P Cardoso, D E Cox, T A Hewston, B L Chamberland *J. Solid State Chem.* **72** 234 (1988)
24. J B Goodenough, G Dutta, A Manthiram *Phys. Rev. B* **43** 10170 (1992)
25. K Imai, H Sawa, M Koike, M Hasegawa, H Takei *J. Solid State Chem.* **114** 184 (1995)
26. H Takei, M Koike, K Imai, H Sawa, H Kadowaki, Y Iye *Mater. Res. Bull.* **27** 555 (1992)
27. L A Picciotto, M M Thackeray, W I F David, P G Bruce, J B Goodenough *Mater. Res. Bull.* **19** 1497 (1984)
28. L A Picciotto, M M Thackeray *Solid State Ion.* **18–19** 773 (1986)
29. J B Goodenough, A Manthiram, G Dutta *Eur. J. Solid State Inorg. Chem.* **28** 1125 (1991)
30. L A Picciotto, M M Thackeray *Mater. Res. Bull.* **20** 187 (1985)
31. C Chieh, B L Chamberland, A F Wells *Acta Crystallogr., Sect. B* **37** 1813 (1981)
32. C Simo, S L Holt *J. Solid State Chem.* **4** 76 (1972)
33. L Hernan, M Macias, J Morales, C Perez-Vicente, J L Tirado *Mater. Res. Bull.* **24** 781 (1989)
34. W D Johnston, R R Heikes *J. Am. Chem. Soc.* **78** 3255 (1956)
35. G Ditrich, R Hoppe *Z. Anorg. Allg. Chem.* **368** 262 (1969)
36. R Hoppe, G Brachtel, M Jansen *Z. Anorg. Allg. Chem.* **417** 1 (1975)
37. P Strobel, J Levy, J-C Joubert *J. Cryst. Growth* **66** 257 (1984)
38. J D Dunitz, L E Orgel *J. Phys. Chem. Solids* **3** 20; 318 (1957)
39. D G Kellerman, V S Gorshkov, V G Zubkov, V A Perelyaev, V R Galakhov, E Z Kurmaev, St Uhlenbrock, M Noimann *Zh. Neorg. Khim.* **42** 1012 (1997) [a]
40. L Croguennec, P Deniard, R Brec, A Lecerf *J. Mater. Chem.* **5** 1919 (1995)
41. L Croguennec, P Deniard, R Brec, P Biensan, M Broussely *Solid State Ion.* **89** 127 (1996)
42. L Croguennec, P Deniard, R Brec, A Lecerf *J. Mater. Chem.* **7** 511 (1997)
43. M M Thackeray, W I F David, P G Bruce, J B Goodenough *Mater. Res. Bull.* **18** 461 (1983)
44. A Mosbah, A Verbnere, M Tournoux *Mater. Res. Bull.* **18** 1375 (1983)
45. A R Armstrong, P G Bruce *Nature (London)* **381** 499 (1996)
46. J N Reimers, J E W Fuller, E Rossen, J R Dahn *J. Electrochem. Soc.* **140** 3396 (1993)
47. R J Gummow, M M Thackeray *J. Electrochem. Soc.* **141** 1178 (1994)
48. C Delmas, F Capitaine, in *Extended Abstracts II-B-33 of the 8th International Meeting on Lithium Batteries, Nagoya, 1996* p. 470
49. F Capitaine, P Gravereau, C Delmas *Solid State Ion.* **89** 197 (1996)
50. Y Shao-Horn, S A Hackney, A R Armstrong, P G Bruce, R Gitzendanner, C S Johnson, M M Thackeray *J. Electrochem. Soc.* **146** 2404 (1999)
51. G Ceder, S K Mishra. *Electrochem. Solid State Lett.* **2** 550 (1999)
52. F Le Gras, P Strobel, M Anne, D Bloch *J. Mater. Chem.* **7** 2519 (1997)
53. J C Anderson, S M Anderson *J. Phys. Chem. Solids* **25** 961 (1964)
54. E Posnjak, T Barth *Phys. Rev.* **38** 2234 (1931)
55. A Hoffman *Naturwissenschaften* **26** 431 (1938)
56. R Famery, P Bassoul, F Queyroux *J. Solid State Chem.* **57** 178 (1985)
57. J C Anderson, S K Dey, V Halpern *J. Phys. Chem. Solids* **26** 1555 (1965)
58. R W G Wykoff *Crystal Structure* Vol. 2 (New York: Intrscience, 1964) p. 312
59. M Brunel, F de Bergevin *J. Phys. Chem. Solids* **29** 163 (1968)
60. M Brunel, F de Bergevin *J. Phys. Chem. Solids* **30** 2011 (1969)
61. J C Anderson, M Schieber *J. Phys. Chem.* **67** 1838 (1963)
62. R Kanno, T Shirane, Y Kawamoto, Y Takeda, M Takano, M Ohashi, Y Yamaguchi *J. Electrochem. Soc.* **143** 2435 (1996)
63. Y Sakurai, H Arai, S Okada, J Yamaki *J. Power Sources* **68** 711 (1997)
64. Y Sakurai, H Arai, J Yamaki *Solid State Ion.* **113–115** 29 (1998)
65. R Kanno, T Shirane, Y Inaba, Y Kawamoto *J. Power Sources* **68** 145 (1997)
66. Y Inaba, Y Kawamoto, in *Extended Abstracts I-B-04 of the 22nd Symposium on Solid State Ionics, Nagoya, 1996* p. 53
67. E Antolini, M Ferretti *J. Solid State Chem.* **117** 1 (1995)
68. H J Orman, P J Weisman *Acta Crystallogr., Sect. C* **40** 12 (1984).
69. W D Johnston, R R Heikes, D Sestrich *J. Phys. Chem. Solids* **7** 1 (1958).
70. J Akimoto, Y Gotoh, Y Oosawa *J. Solid State Chem.* **141** 298 (1998)
71. C Wolverton, A Zunger *Phys. Rev. B* **57** 2242 (1998)
72. C Wolverton, A Zunger *J. Electrochem. Soc.* **145** 2424 (1998)
73. R J Gummow, M M Thackeray *Solid State Ion.* **53–56** 681 (1992)
74. R J Gummow, M M Thackeray *J. Electrochem. Soc.* **140** 3365 (1993)
75. R J Gummow, D C Liles, M M Thackeray *Mater. Res. Bull.* **28** 235 (1992)
76. R J Gummov, D C Liles, M M Thackeray, W I F David *Mater. Res. Bull.* **28** 1177 (1993)
77. E Rossen, J N Reimers, J R Dahn *Solid State Ion.* **62** 53 (1993)
78. J Morales, R Stoyanova, J L Tirado, E Zhecheva *J. Solid State Chem.* **113** 182 (1994)
79. B Garcia, P Barboux, F Ribot, A Kihn-Hirari, L Mazerolles, N Baffier *Solid State Ion.* **80** 111 (1995)

80. W W Huang, R Frech *Solid State Ion*. **86** – **88** 395 (1996)
81. G G Amatucci, J M Tarascon, D Larcher, L C Klein *Solid State Ion*. **84** 169 (1996)
82. M Carewska, S Scaccia, F Croce, S Arumugam, Y Wang, S Greenbaum *Solid State Ion*. **93** 227 (1997)
83. Y Shao-Horn, S A Hackney, S C Johnson, A J Kahaian, M M Thackeray *J. Solid State Chem*. **140** 116 (1998)
84. J N Reimers, J R Dahn *J. Electrochem. Soc*. **139** 2091 (1992)
85. T Ohzuku, A Ueda *J. Electrochem. Soc*. **141** 2972 (1994)
86. G G Amatucci, J M Tarascon, L C Klein *J. Electrochem. Soc*. **143** 1114 (1996)
87. A van der Ven, M K Aydinol, G Ceder, G Kresse, J Hafner *Phys. Rev. B* **58** 2975 (1998)
88. A van der Ven, M K Aydinol, G Ceder *J. Electrochem. Soc*. **145** 2149 (1998)
89. B Garcia, J Farcy, J P Pereira-Ramos, N Baffier *J. Electrochem. Soc*. **144** 1179 (1997)
90. A Mendiboure, C Delmas, P Hagenmuller *Mater. Res. Bull*. **19** 1383 (1984)
91. C Delmas, J Braconnier, P Hagenmuller *Mater. Res. Bull*. **17** 117 (1982)
92. N Imanishi, M Fujiyoshi, Y Takeda, O Yamamoto, M Tabuchi *Solid State Ion*. **18** 121 (1999)
93. L D Dyer, B S Borie, G P Smith *J. Am. Chem. Soc*. **76** 1499 (1953)
94. A Rougier, C Delmas, A V Chadwick *Solid State Commun*. **94** 121 (1995)
95. A Rougier, A V Chadwick, C Delmas *Nucl. Instum. Methods Phys. Res*. **97** 75 (1995)
96. J B Goodenough, D G Wickham, W J Croft *J. Phys.Chem. Solids* **5** 107 (1958).
97. V S Gorshkov, D G Kellerman, V A Perelyaev, G P Shveikin *Izv. Akad Nauk SSSR, Neorg. Mater*. **27** 1274 (1991) [b]
98. V S Gorshkov, D G Kellerman, V A Perelyaev, G P Shveikin *Zh. Neorg. Khim*. **41** 16 (1996) [a]
99. Z Lu, X Huang, H Huang, L Chen, J Schoonman *Solid State Ion*. **120** 103 (1999)
100. E Antolini *J. Mater. Sci*. **27** 3335 (1992)
101. E Antolini *J. Mater. Sci. Lett*. **13** 1599 (1994)
102. T Sata *Ceram. Int*. **24** 53 (1998)
103. H Arai, S Okada, H Ohtsuka, M Ichimura, J Yamaki *Solid State Ion*. **80** 261 (1995)
104. V Berbenni, V Massarotti, D Capsoni, R Riccardi, A Marini, E Antolini *Solid State Ion*. **48** 101 (1991)
105. J Morales, C Perez-Vicente, J L Tirado *Mater. Res. Bull*. **25** 623 (1990)
106. W Li, J N Reimers, J R Dahn *Phys. Rev. B* **46** 3236 (1992)
107. A Rougier, P Gravereau, C Delmas *J. Electrochem. Soc*. **143** 1168 (1996)
108. I J Pickering, J T Lewandowski, A J Jacobson, A Goldstone *Solid State Ion*. **53** – **56** 405 (1992)
109. J N Reimers, W Li, J R Dahn *Phys. Rev. B* **47** 8486 (1993)
110. R Alcantara, P Lavela, J L Tirado, R Stoyanova, E Kuzmanova, E Zhecheva *Chem. Mater*. **9** 2145 (1997)
111. I J Pickering, G N George, J T Lewandowski, A J Jacobson *J. Am. Chem. Soc*. **115** 4137 (1993)
112. T Ohzuku, A Ueda, M Nagayama *J. Electrochem. Soc*. **140** 1862 (1993)
113. I Nakai, K Takahashi, Y Shiraishi, T Nakagome, F Nishikawa *J. Solid State Chem*. **140** 145 (1998)
114. L Croguennec, C Pouillerie, C Delmas *Solid State Ion*. **135** 259 (2000)
115. A Hirano, R Kanno, Y Kawamoto, Y Takeda, K Yamaura, M Takano, K Ohyama, M Ohashi, Y Yamaguchi *Solid State Ion*. **78** 123 (1995)
116. R Stoyanova, E Zhecheva *J. Solid State Chem*. **108** 211 (1994)
117. A Hirano, R Kanno, Y Kawamoto, K Oikawa, T Kamiyama, F Izumi *Solid State Ion*. **86** – **88** 791 (1996)
118. C Delmas, J P Peres, A Rougier, A Demourgues, F Weill, A V Chadwick, M Broussely, F Perton, P Biensan, P Willmann *J. Power Sources* **68** 120 (1997)
119. J P Peres, F Weill, C Delmas *Solid State Ion*. **116** 19 (1999)
120. H Arai, S Okada, Y Sakurai, J-i Yamaki *Solid State Ion*. **109** 295 (1998)
121. J R Dahn, U von Sacken, C A Michal *Solid State Ion*. **44** 87 (1990)
122. V W Bronger, H Bade, W Klemm *Z. Anorg. Allg. Chem*. **333** 188 (1964)
123. H N Migeon, A Courtois, M Zanne, C Cleitzer *Rev. Chim. Miner*. **13** 1 (1976)
124. P F Bongers, in *Crystal Structure and Chemical Bonding in Inorganic Chemistry* (Eds C J M Rooymans, A Rabenau) (New York: Elsevier, 1975) p. 246
125. J B Goodenough *Magnetism and the Chemical Bond* (New York, London: Wiley-Interscience, 1963)
126. Y Kimishima, M Tsuchiya, K Tomimoto, J Akimitsu *J. Magn. Magn. Mater*. **104** – **107** 779 (1992)
127. H F Pen, L H Tjeng, E Pellegrin, F M F de Groot, G A Sawatsky, M A van Veendaal, C T Chen *Phys. Rev. B* **55** 15500 (1997)
128. N F Mott *Metal-Insulator Transition* (London: Taylor and Francis, 1974)
129. Ya V Vasil'ev, S M Ariya *Izv. Akad. Nauk SSSR, Neorg. Mater*. **1** 347 (1965) [b]
130. A A Bugaev, B P Zakharchenya, F A Chudnovskii *Fazovyi Perekhod Poluprovodnik – Metall i ego Primenenie* (Semiconductor – Metal Phase Transition and Its Application) (Leningrad: Nauka, 1979)
131. D G Kellerman, V S Gorshkov, V A Perelyaev *Izv. Akad. Nauk SSSR, Neorg. Mater*. **24** 1547 (1988) [b]
132. M Onoda, T Inabe *J. Phys. Soc. Jpn*. **62** 2216 (1993)
133. B Laar, D J Ijdo *J. Solid State Chem*. **3** 590 (1971)
134. M Krysowska *Acta Phys. Pol. A* **52** 97 (1977)
135. C Delmas, G Le Flem, C Fouassier, P Hagenmuller *J. Phys. Chem. Solids* **39** 55 (1978)
136. N Kojima, K Ito, I Mogi, M Takeda, G Kido,Y Nakagawa, M Sakai, N Kuroda, Y Nishina *J. Phys. Soc. Jpn*. **62** 4137 (1993)
137. J L Soubeyboux, D Fruchart, J C Marmeggi, W J Fitzgerald, C Delmas, G Le Flem *Phys. Status Solidi A* **67** 633 (1981).
138. M Suzuki, I Yamada, H Kadowaki, F Takei *J. Phys., Condens. Matter* **5** 4225 (1993)
139. Y Ajiro, H Kikuchi, S Sugiyama, T Nakashima, S Shamoto, N Nakayama, M Kiyama, N Yamamoto, Y Oka *J. Phys. Soc. Jpn*. **57** 2268 (1988)
140. H Kadowaki, H Takei, K Motoya *J. Phys., Condens. Matter* **7** 6869 (1995)
141. J E Greedan, N P Raju, I J Davidson *J. Solid State Chem*. **128** 209 (1997)
142. V S Gorshkov, V V Karelina, D G Kellerman, in *Oksidy. Fiziko-Khimicheskie Svoistva i Tekhnologiya (Tez. Dokl. Vserossiiskoi Nauchno-Prakticheskoi Konf.)* [Oxides. Physicochemical Properties and Technology (Abstracts of Reports of the All-Russian Scientific and Practical Conference)] (Ekaterinburg: Ural Branch of the Russian Academy of Sciences, 1999) p. 157
143. D E Cox, G Shirane, P A Flinn, S L Ruby, W J Takei *Phys. Rev., Ser. 2* **132** 1547 (1963)
144. M Tabuchi, K Ado, H Kobayashi, I Matsubara, H Kageyama, M Wakita, S Tsutsui, S Nasu, Y Takeda, C Masquelier, A Hirano, R Kanno *J. Solid State Chem*. **141** 554 (1998)
145. M Tabuchi, S Tsutsui, C Masquelier, R Kanno, K Ado, I Matsubara, S Nasu, H Kageyama *J. Solid State Chem*. **140** 159 (1998)
146. M Oku *J. Solid State Chem*. **23** 177 (1978)
147. V S Gorshkov, D G Kellerman, V V Karelina *Zh. Fiz. Khim*. **73** 1041 (1999) [c]
148. R Stoyanova, E Zhecheva, C Friebel *Solid State Ion*. **73** 1 (1994)
149. G F Dionne *J. Appl. Phys*. **67** 4561 (1990)
150. K Hirakawa, H Kadwaki, K Ubukoshi *J. Phys. Soc. Jpn*. **54** 3256 (1985)
151. P Kuiper, G Kruizinga, J Ghijsen, G A Sawatsky, H Verweij *Phys. Rev. Lett*. **62** 221 (1989)
152. V R Galakhov, E Z Kurmaev, S Uhlenbrock, M Neumann, D G Kellerman, V S Gorshkov *Solid State Commun*. **95** 347 (1995)
153. T Mizokawa, H Namatame, A Fujimori, K Akeyama, H Kondoh, H Kuroda, N Kosugi *Phys. Rev. Lett*. **67** 1638 (1991)
154. J Meng, P Jena, J M Vail *J. Phys., Condens. Matter* **2** 10371 (1990)
155. P Ganguly, V Ramaswamy, I S Mulla, R F Shinde, P P Bakare, S Ganapathy, P R Rajamohanan, N V K Prakash *Phys. Rev. B* **46** 11595 (1992)
156. P W Anderson *Mater. Res. Bull*. **8** 153 (1973)

157. P W Anderson *Science* **235** 1196 (1987)
158. M Itoh, I Yamada, K Ubukoshi, K Hirakawa, H Yasuoka *J. Phys. Soc. Jpn.* **55** 2125 (1986)
159. I Yamada, K Ubukoshi, K Hirakawa *J. Phys. Soc. Jpn.* **54** 3571 (1985)
160. K Yamaura, M Takano, A Hirano, R Kanno *J. Solid State Chem.* **127** 109 (1996)
161. J P Kemp, P A Cox, J W Hodby *J. Phys., Condens. Matter* **2** 6699 (1990)
162. T Shirakami, M Takematsu, A Hirano, R Kanno, K Yamaura, M Takano, T Atake *Mater. Sci. Eng. B* **54** 70 (1998)
163. H Yoshikawa, H Mori, K Hirota, M Ishikawa *J. Phys. Soc. Jpn.* **59** 2631 (1986)
164. K Hirota, Y Nakazawa, M Ishikawa *J. Phys., Condens. Matter* **3** 4721 (1991)
165. K Hirota, Y Nakazawa, M Ishikawa *J. Magn. Magn. Mater.* **90 – 91** 279 (1990)
166. K Hirakawa, H Kadwaki *Physica B* **136** 335 (1986)
167. M E Fisher *Rep. Prog. Phys.* **30** 615 (1967)
168. D Mertz, Y Ksari, J Celestini, J M Debierre, A Stepanov, C Delmas *Phys. Rev. B* **61** 1240 (2000)
169. A-L Barra, G Chouteau, A Stepanov, C Delmas *J. Magn. Magn. Mater.* **177 – 181** 783 (1998)
170. P Ganguly *Proc. Indian Natl. Sci. Acad. A* **52** 13 (1986)
171. J N Reimers, J R Dahn, J E Greedan, C V Stager, G Liu, I Davidson, U von Sacken *J. Solid State Chem.* **102** 542 (1993)
172. L J de Jongh, A R Miedema *Adv. Phys.* **23** 1 (1974)
173. J H P Colpa *Physica B* **57** 347 (1972)
174. R Kanno, H Kubo, Y Kawamoto, T Kamiyama, F Izumi, Y Takeda, M Takano *J. Solid State Chem.* **110** 216 (1994)
175. C Delmas, I Saadoune *Solid State Ion.* **53** 370 (1992)
176. Y-M Choi, S-I Pyun, S-I Moon *Solid State Ion.* **89** 43 (1996)
177. A Rougier, I Saadoune, P Gravereau, P Willmann, C Delmas *Solid State Ion.* **90** 83 (1996)
178. I Saadoune, C Delmas *J. Solid State Chem.* **136** 8 (1998)
179. R Alcantara, J Morales, J L Tirado, R Stayanova, E Zhecheva *J. Electrochem. Soc.* **142** 3997 (1995)
180. Y Fujita, K Amine, J Maruta, H Yasuda *J. Power Sources* **68** 126 (1997)
181. J Cho, G Kim, H S Lim *J. Electrochem. Soc.* **146** 3571 (1999)
182. C-C Chang, N Scarr, P N Kumta *Solid State Ion.* **112** 329 (1998)
183. S Tao, Q Wa, Z Zhan, G Meng *Solid State Ion.* **124** 33 (1999)
184. C Julien, S S Michael, S Ziolkievicz *Int. J. Inorg. Mater.* **1** 29 (1999)
185. D Caurant, N Baffer, B Garcia, J P Pereira-Ramos *Solid State Ion.* **91** 45 (1996)
186. M Menetrier, A Pougier, C Delmas *Solid State Commun.* **90** 439 (1994)
187. C Marichal, J Hirschinger, P Granger, M Menetrier, A Rougier, C Delmas *Inorg. Chem.* **34** 1773 (1995)
188. K Hirota, H Yoshikawa, M Ishikawa *J. Phys., Condens. Matter* **4** 6291 (1992)
189. Z L Liu, A S Yu, J Y Lee *J. Power Sources* **82** 416 (1999)
190. Y Cao, M V Yakovleva, W B Ebner *Electrochem. Solid State Lett.* **1** 117 (1998)
191. H-J Kweon, D G Park *Electrochem. Solid State Lett.* **3** 128 (2000)
192. H S Chang, S-G Kang, S-W Song, J-B Yoon, J-H Choy *Solid State Ion.* **86 – 88** 171 (1996)
193. M E Spahr, P Novak, B Schnayder, O Haas, R Nesper *J. Electrochem. Soc.* **145** 1113 (1998)
194. S Fujiwara, S Yamada, M Kanda, in *Extended Abstracts of the 34th Battery Symposium, Nagoya, 1993* p. 135
195. M Yoshio, K Yamata, J Itoh, H Noguchi, M Okada, T Mouri, in *Rechargeable Lithium and Lithium Ion Batteries* (Eds S Megahed, B M Barnett, L Xie) (Pennington, NJ: Electrochemical Society, 1995) p. 251
196. Y Nitta, K Okamura, K Haraguchi, S Kobayashi, A Ohta *J. Power Sources* **54** 511 (1995)
197. E Rossen, C D W Jones, J R Dahn *Solid State Ion.* **57** 311 (1992)
198. D Caurant, N Baffier, V Bianchi, G Gregoire, S Bach *J. Mater. Chem.* **6** 1149 (1996)
199. J M Paulsen, C L Thomas, J R Dahn *J. Electrochem. Soc.* **147** 861 (2000)
200. D G Kellerman, V S Gorshkov, V A Perelyaev, G P Shveikin *Zh. Neorg. Khim.* **35** 1267 (1990) [b]
201. D G Kellerman, V S Gorshkov, V V Karelina *Zh. Neorg. Khim.* **44** 1078 (1999) [b]
202. C Delmas, G Prado, A Rougier, E Suard, L Fournes *Solid State Ion.* **135** 71 (2000)
203. J N Reimers, E Rossen, C D Jones, J R Dahn *Solid State Ion.* **61** 335 (1993)
204. R Stoyanova, E Zhecheva, L Zarkova *Solid State Ion.* **73** 233 (1994)
205. K Numata, C Sakaki, S Yamanaka *Solid State Ion.* **117** 257 (1999)
206. M Jansen, R Hoppe *Z. Anorg. Allg. Chem.* **397** 279 (1972)
207. F Zang, M S Whittingham *Electrochem. Solid State Lett.* **3** 309 (2000)
208. A Tauber, W M Moller, E Banks *J. Solid State Chem.* **4** 138 (1972)
209. E Kordes, J Petzoldt *Z. Anorg. Allg. Chem.* **335** 138 (1965)
210. C Delmas, F Menil, G Flem, C Fouassier, P Hagenmuller *J. Phys. Chem. Solids* **39** 51 (1978)
211. T Naka, M Onoda, H Nagasawa *Solid State Commun.* **87** 679 (1993)
212. T Ohzuku, T Yanagawa, M Kouguchi, A Ueda *J. Power Sources* **68** 131 (1997)
213. G X Wang, S Zhong, D H Bradhurst, S X Dou, H K Liu *Solid State Ion.* **116** 271 (1999)
214. S Buta, D Morgan, A van der Ven, M K Aydinol, G Ceder *J. Electrochem. Soc.* **146** 4335 (1999)
215. H-A Lehman, H Hesselbarth *Z. Anorg. Allg. Chem.* **313** 117 (1961)
216. G Chen, W Hao, Y Shi, Y Wu, S Perkowitz *J. Mater. Res.* **15** 583 (2000)
217. R Stoyanova, E Zhecheva, E Kuzmanova, R Alcantara, P Lavela, J L Tirado *Solid State Ion.* **128** 1 (2000)
218. K R Poeppelmeier, S H Thong *J. Less-Common Met.* **156** 191 (1989)
219. Y I Jang, Y M Chiang *Solid State Ion.* **130** 53 (2000)
220. B Ammundsen, J Desilvestro, T Groutso, D Hassell, J B Metson, E Regan, R Steiner, P J Pickering *J. Electrochem. Soc.* **147** 4078 (2000)
221. C D W Jones, E Rossen, J R Dahn *Solid State Ion.* **68** 65 (1994)
222. H Kobayashi, H Shigemura, M Tabuchi, H Sakaebe, K Ado, H Kageyama, A Hirano, R Kanno, M Wakita, S Morimoto, S Nasu *J. Electrochem. Soc.* **147** 960 (2000)
223. C Julien, G A Nazri, A Rogier *Solid State Ion.* **135** 121 (2000)
224. Yu D Tret'yakov, O A Brylev *Ros. Khim. Zh.* **44** 10 (2000) [d]
225. C A Vincent *Solid State Ion.* **134** 159 (2000)

[a] — *Russ. J. Inorg. Chem. (Engl. Transl.)*
[b] — *Inorg. Mater. (Engl. Transl.)*
[c] — *Russ. J. Phys. Chem. (Engl. Transl.)*
[d] — *Mendeleev Chem. J. (Engl. Transl.)*